RAY TRACING STUDY OF IONOSPHERIC EFFECTS ON HF AND VHF RADIO WAVES

By

R. P. PANDEY (CAPTAIN)

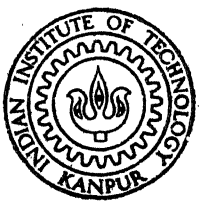

DEPARTMENT OF ELECTRICAL ENGINEERING

INDIAN INSTITUTE OF TECHNOLOGY KANPUR

JULY 1974

RAY TRACING STUDY OF IONOSPHERIC EFFECTS ON HF AND VHF RADIO WAVES

A Thesis Submitted
In Partial Fulfilment of the Requirements
for the Degree of

MASTER OF TECHNOLOGY

By

R. P. PANDEY (CAPTAIN)

to the

DEPARTMENT OF ELECTRICAL ENGINEERING
INDIAN INSTITUTE OF TECHNOLOGY KANPUR

JULY 1974

CERTIFICATE

This is to certify that the thesis entitled 'Ray Tracing Study of Ionospheric Effects on HF and VHF Radio Waves' is a record of the work carried out under my supervision and that it has not been submitted elsewhere for a degree.

Dr. N.C. Mathur
Professor
Department of Electrical Engineering
Indian Institute of Technology
Kanpur

Kanpur
July 1974.

CERTIFICATE

This is to certify that the thesis entitled 'Ray Tracing Study of Ionospheric Effects on HF and VHF Radio Waves' is a record of the work carried out under my supervision and that it has not been submitted elsewhere for a degree.

N C Mathur

Dr. N.C. Mathur
Professor
Department of Electrical Engineering
Indian Institute of Technology
Kanpur

Kanpur
July 1974.

ACKNOWLEDGEMENT

I am deeply indebted to my thesis supervisor, Professor N.C. Mathur, for constant help and encouragement throughout this work. I also thank him for his valuable suggestions provided despite his busy schedule.

Thanks are also due to Staff of the Computer Center for their valuable help. Finally, Mr. K.N.Tewari deserves special mention for his excellent and neat typing work.

R.P. PANDEY
(CAPTAIN)

TABLE OF CONTENTS

ABSTRACT

In this thesis certain aspects of radio wave propagation through the ionosphere are investigated with the help of ray tracing using a digital computer for the purpose. A computerised three dimensional ray tracing program is used based upon the Haselgrove equations and employing the Appleton-Hartree equation for the index of refraction. The program is based on the work of Jones (1966). This routine has been used to predict the effect of elevation angle and frequency of transmission upon ground distance, maximum height of reflection, various path lengths and ray path trajectories of HF and VHF radio waves through regular and disturbed ionosphere with and without considering the effect of imposed magnetic field. Effects of collision are not presented in this paper. A North-South propagation path along constant geomagnetic longitude is considered. The transmitter is located at Kanpur (26.5°N, 80.5°E) and receiver is either on ground or on a satellite at height of 1000 Km above ground.

Suitable models for earth's magnetic field, ionospheric electron density and perturbation to the ionospheric electron density have been used. A Gaussian perturbation (torus) to the ionospheric electron density model has been introduced for this work. The

basic features of the ionospheric irregularities and phase path characteristics for oblique ray paths are reviewed along with the underlying theory of the ionospheric ray tracing algorithms.

The result of this simulation indicate that in general:

(i) Ray path trajectories are significantly affected in the vicinity of torus, the rays whose wave reversal occur near the center of the torus are the most significantly affected.

(ii) Ray path symmetry about the point of reflection is not disturbed appreciably.

(iii) There is significant change in various path lengths and skip distance.

(iv) The highly non-concentric isoelectron contours caused by the presence of the torus may result in significant large scale focussing/defocussing of the radio waves. In general, ray reflected from the center portion of the torus are focussed.

(v) For any undisturbed ionospheric electron density profile and signal transmission frequency above critical frequency, a cusp is observed in a curve depicting variation of phase path length

and ground range with elevation angle, whereas a nose appears in a curve depicting variation of group path length and ground range with elevation angle. In former case the slope of the curve changes gradually whereas in the latter case the slope of the curve changes abruptly.

Chapter 1

INTRODUCTION

1.1 General[3,7,12]

Ray tracing is a technique of finding the path followed by radio waves from transmitter to receiver through an ionized medium in terms of geometrical optics. For ionospheric problems, ray tracing can be used to determine such basic parameters as the direction of energy flow, ground range, maximum height of reflection, phase path, group path, actual path length etc. From these basic data, many other desired quantities can then be deduced. A three dimensional ray tracing program developed by R.M.Jones of ESSA (1968) written in CDC 3600 FORTRAN,which is similar to FORTRAN IV is used to trace radio rays through the ionosphere. This could be converted to other applications by substituting an appropriate index of refraction subroutine.

Since the first years of ionospheric studies, as early as 1920's, certain forms of ray tracing have been used for ionospheric problems which involved laborious calculations so as to get an idea of refraction according to the laws of geometrical optics but within the past decade the increasing availability of high-speed digital computers has greatly stimulated

the development and application of ray tracing process by permitting extensive use of voluminous and complex calculations which earlier could be done only in rare cases and at the expense of much time and labour.

1.2 Need for Ray Tracing

To determine the amplitude, polarization, relative phase, time of flight, absorption, Doppler frequency shift, skip distance, maximum usable frequency (MUF), etc. of a radio wave, it is necessary to determine the ray path between transmitter and receiver. At first glance, it might appear that it is easy to determine the path along which the energy flows. However, this is not the case in practice. For a few simple ionospheric electron density N(h) profiles, in which electron collisions, the earth's magnetic field and ionospheric irregularities are neglected, it is possible to determine ray path analytically. In general, however, the paths have to be determined by a step-by-step process. There are varying degrees of sophistication in ray tracing. In simplest form of ray tracing the ionosphere is considered as a plane mirror, and ray paths are made up of linear segments. In more sophisticated ray tracing programs the effects of electron-density variations (sufficiently slow for ray theory to hold), magnetic-field changes, collision frequency, perturbation to the electron deisity are all taken into account.

1.3 Scope

Ray tracing techniques can be accurately and efficiently employed for studying radio ray path trajectories in ionosphere and troposphere at HF band, ionospheric phase distortion at UHF band and other effects such as absorption, Doppler frequency shift, bearing deviation, error in angle of transmission, etc. This work makes use of ray tracing techniques to study such parameters as ground range, phase path, group path, etc. for various elevation angles and frequencies of transmission in HF and VHF band. Studies have been made both with and without the effect of imposed magnetic field of the earth. The effect of collision has not been considered. However, the same can be included by using suitable collision frequency model to estimate absorption. An analytical model of electron density has been used to represent the electron density contours. A perturbation model is used to represent the effect of torus upon the electron density contours. Since the primary objective of introducing perturbation is to deduce order-of-magnitude characteristics of the ray path trajectories, the presence of the earth's magnetic field has been neglected while studying the effect of perturbation. Ray path trajectories and phase path characteristics for oblique angle rays have been plotted by IBM 1800 computer to depict effect of elevation angle and frequency of transmission through a regular as well as perturbed ionosphere.

Chapter 2

IONOSPHERE

2.1 Ionospheric Structure[3]

The ionosphere is that region of the earth's atmosphere lying approximately between 50 Km and one earth radius (6370 Km), in which sufficient ionization exists to enfluence the propagation of radio waves. The ionosphere is sub-divided into D,E and F regions within which layers of electrons exist.The chief characteristic of each layer is the critical frequency which is the highest frequency reflected by the layer for vertical incidence. It depends upon the electron density.

2.1.1 Regions and Layers:

The approximate locations of regions and the layers that may exist within them are given in Table 2.1 below.

TABLE 2.1

Region	Height Km	Layer	Approximate height,Km	Approximate Day time Electron Density m^{-3}
D	50-90	C	65	10^8
		D	75-80	10^9
E	90 to 120-140	E1	110	10^{11}
		E_s	100	Unpredictable
F	120-140 and above	F1, F1½	200	2×10^{11}
		F2	above 250	10^{12}

C-layer (50-70 Km) is produced by cosmic rays, whereas the other layer,are produced by solar radiations, with the exception of sporadic E layer (E_s) which is produced by meteoric particles. D-layer exists in daytime with its maximum electron density near 80 Km with an average thickness of 10 Km. In D-layer degree of ionization depends on the altitude of sun and therefore it disappears at night. El-layer is always present by day in all seasons and in all geographical locations and its behaviour is subject to close solar control. The sporadic E-layer (E_s) consist largely of relatively dense patches of electrons of the order of a few tens of kilometers in horizontal extent. The critical frequency of E-layer is given by

$$f_oE = 0.9[(180 + 1.44R) \cos \chi]^{0.25} \qquad (2.1)$$

where R is Zurich sunspot number (SSN) and χ is Zenith angle.

Fl-layer (200-250 Km) with day time average thickness of 20 Km, combines with F2-layer at night. It undergoes seasonal as well as solar cycle variations. It is more pronounced during summer than during winter and at high sunspot number. The critical frequency of Fl-layer is given by

$$f_oFl = (4.3 + 0.01R) \cos^{0.2}\chi \qquad (2.2)$$

To a first approximation the exponent in equation (2.2) varies from place to place and with season. It is less during sunspot minimum than at sunspot maximum. F2-layer (200-400 Km) is by far the most important reflecting medium for HF radio waves. At night it falls to a height of 300 Km and combines with F1-layer. Its height and ionization density vary largely, and depend on sunspot cycle and undergo diurnal and seasonal variations. Its critical frequency varies linearly with SSN (for R = 0 to 150) and thereafter it flattens out. It is given by

$$f_oF2 = 5.4(1 + 0.0064R) \qquad (2.3)$$

2.1.2 A Chapman Layer:

E and F layers are not very distinct and with sufficient accuracy it can be assumed that during day light hours E-layer is a Chapman layer and obeys the law as given below.

$$N = N_o \exp \tfrac{1}{2}[1-z-\sec \chi \exp(-z)] \qquad (2.4)$$

where

$$z = \frac{h - h_o}{H}$$

χ = Zenith angle

H = scale height

h = height where electron density is computed in relation (2.4)

h_o = height of maximum ion production when sun is overhead, Reference height.

The critical frequency of E-layer (with H = 10 Km, h_o = 115 Km, $N_o = 2.8 \times 10^5$ (m^{-3}) is $4.7(\cos \chi)^{1/4}$ MHz during day and is of the order of 0.5 MHz at night.

2.2 Ray Paths in the Ionosphere

A radio wave travelling from transmitter (T) to receiver (R) through ionosphere along a curved path is depicted in Figure 2.1. The basic expressions for phase path (P), group path (P') and ground range (D) are

$$P = \int_T^R \mu \, ds$$

$$P' = \int_T^R \mu' \, ds \qquad (2.5)$$

$$D = \int_T^R R_o \, d\theta$$

where μ = phase refractive index of the ionosphere

μ' = group refractive index of the ionosphere

$$= \frac{d}{df}(\mu f)$$

$$= \mu + f \frac{d\mu}{df}$$

d_s = an element of path length and

$d\theta$ = angle subtended at the centre of the earth by ds as shown in Figure 2.2.

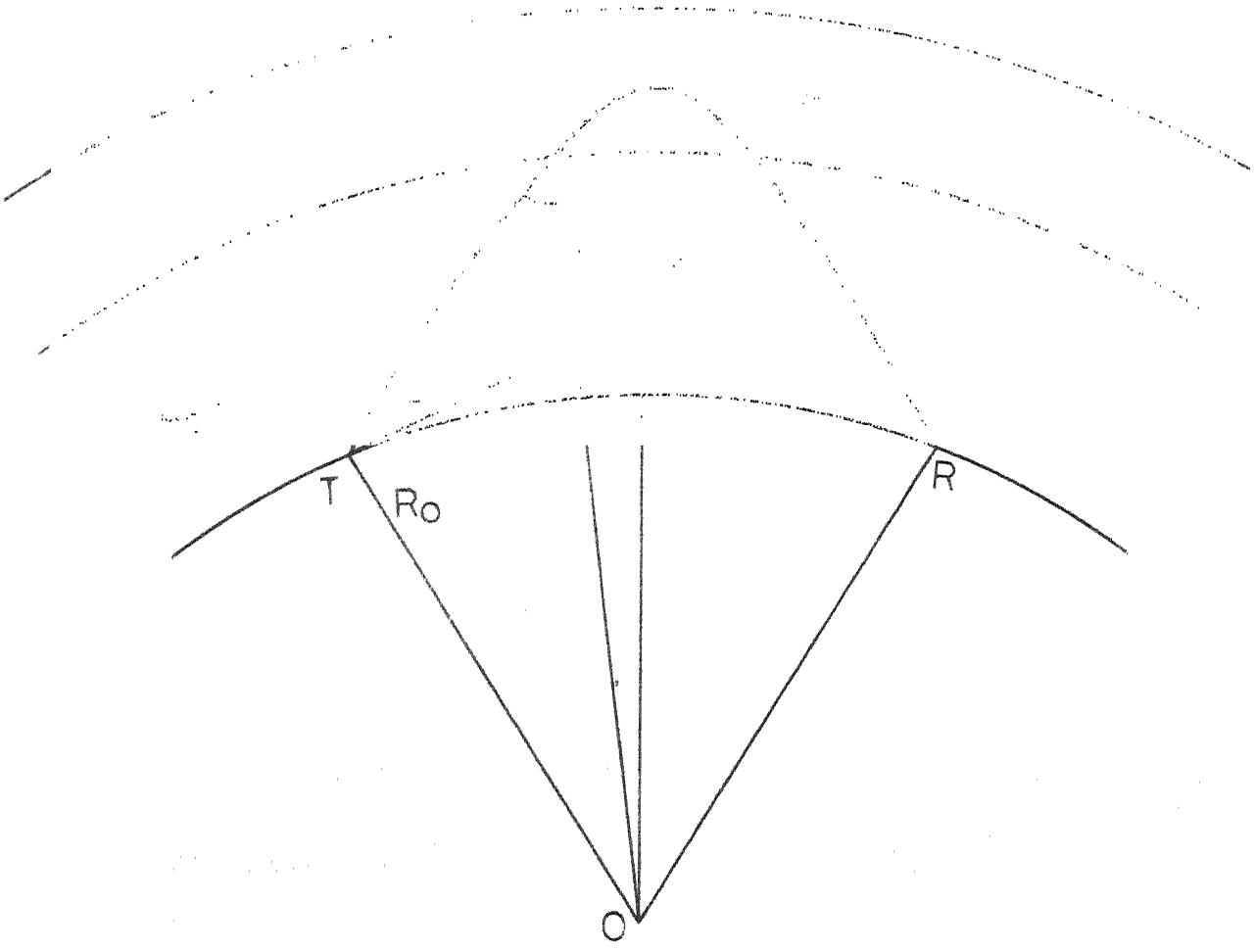

Fig. 2.1

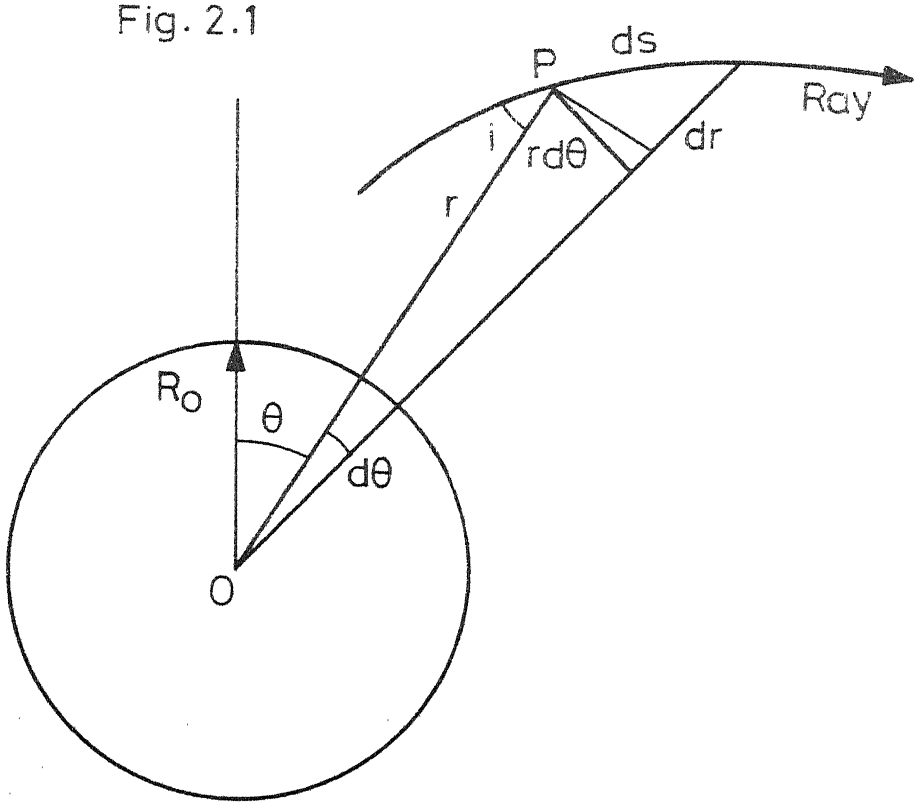

Fig. 2.2

Ray Geometry

Each integral is taken over the entire path between transmitter and receiver. In absence of magnetic field and electron collision, the group refractive index is inverse of phase refractive index.

Applying Bouger's rule[5] to the geometry of Figure 2.1, we have

$$\mu r \sin i = R_o \cos \Delta \tag{2.6}$$

From the ray geometry of Figure 2.2, the elements of angle and length are related by the equations

$$ds = \frac{r\, d\theta}{\sin i} = \frac{dr}{\cos i} \tag{2.7}$$

and therefore, from equations (2.5), (2.6) and (2.7) we get

$$P = \int_T^R \mu \, ds$$

$$= \int_T^R \frac{\mu \, dr}{\cos i} \tag{2.8a}$$

$$= 2 \int_{R_o}^{r_v} \frac{\mu^2 \, r \, dr}{(\mu^2 r^2 - R_o^2 \cos^2 \Delta)^{\frac{1}{2}}}$$

$$P' = \int_T^R \mu' \, ds$$

$$= \int_T^R \frac{ds}{\mu} \tag{2.8b}$$

$$= 2 \int_{R_o}^{r_v} \frac{r \, dr}{(\mu^2 r^2 - R_o^2 \cos^2 \Delta)^{\frac{1}{2}}}$$

$$D = \int_{T}^{R} R_o \, d\theta$$

$$= 2 \int_{R_o}^{r_v} \frac{R_o^2 \cos A \, dr}{r(\mu^2 r^2 - R_o^2 \cos^2 A)^{\frac{1}{2}}} \qquad (2.8c)$$

where r_v is the value of r at the vertex of the path.

2.3 Ionospheric Irregularities[13,14,16-18]

The ionosphere has been under close observation for over 35 years. Until 1953, investigations have been concerned mostly with the study of long-period variations such as diurnal and seasonal changes in certain parameters, in particular, the height and maximum ionization of the main regions (E,F1,F2). During past few years, with the advent of artificial satellites, it has become possible to scan a large section of the ionosphere in a few minutes. This greatly simplifies the study of ionospheric irregularities and much useful information has already been obtained from observations of satellite signals.

2.3.1 Basic Features:

Experimental observations indicate that the ionospheric irregularities are a permanent features of the day light-hours ionosphere. The ionization

enhancement is thought to extend through the entire F2 region and even into D and E layers. The irregularities have an electron density which is typically 10 percent higher than that of its background.

2.3.2 General Characteristics:

Evidence for the existence of much larger irregularities in the F region, with dimensions of several hundred kilometers, was given by Munro (1950, 1958) by comparing ionospheric virtual height records taken at different times and different places. Similar measurements have been made by several workers by observing changes in the time of travel, the amplitude, or the frequency of radio signals received from two or more stations. These observations only reveal the presence of irregularities that are moving horizontally with a mean speed of 500 Km/min. The irregularities generally have horizontal dimensions of a few hundred kilometers. A few isolated irregularities as large as 2000 Km are observed by Chan and Villard (1962). The presence of large scale irregularities in the F region has also been shown by Vitkevitch and Kokurin (1958) and by Lawrence et al (1961) from observations of slow, irregular variations in the

apparant positions of radio stars. The horizontal dimensions of the irregularity were generally between 200 and 400 Km with electron density variations of about one percent.

The presence of large irregularities in the ionosphere was also deduced by Titheridge (1963) from calculations of the number of free electrons between an observer and a satellite, based on measurements of amplitude of signals received from a satellite Explorer 7, recorded at Ardmore (lattitude 37.01° S, longitude 174.98° E) 17 miles Southeast of Auckland from Nov 1960 to Aug 1961.

He found that there was no seasonal or diurnal variations in their occurrence apart from a possible tendency for fewer to be observed in the early morning. Irregularities can occur singly or in groups of similar size or small ones may be superimposed on large ones. The sizes of those observed ranged from 5 to 500 Km.

The total electron content of the irregularities, measured along the line from satellite to the receiver varied from about 8×10^{13} to 15×10^{15} electrons per meter square in winter. The seasonal change was caused by a decrease in the total electron content of the ionosphere from about 2×10^{17} electrons/m^2 in

summer to $1x10^{17}$ electrons/m^2 in winter. In both seasons then, the electron contents of the irregularities varied from about 0.04 to 7 percent of the total electron content of the ionosphere.

Titheridge (1968) found, by comparing the number of irregularities observed using satellites at different heights, that the number of irregularities per unit volume at any height was approximately proportional to the density of the background ionization. This suggested that the percentage fluctuations in the electron density are approximately the same at all heights above 200 Km. The irregularities were found to exist at heights ranging from 180 to 750 Km. The horizontal sizes varied from 75 to 520 Km. The denser irregularities occurred only near the peak of the ionosphere between 250-400 Km. The irregularities lay on a straight line tilted down to the south at an angle of 15 degrees.

2.3.3 Shape:

Titheridge (1963), using the effect of the Zenith angle of the satellite on the calculated content and size of the irregularities, determined their approximate shape. The irregularities were not elongated in the direction of the magnetic field but occurred in the form of horizontal slabs with a

vertical thickness less than one third of the horizontal dimensions. A typical irregularity has the shape of an oblate spheroid.

2.3.4 Direction of Motion[8]:

Investigations into the phenomenon of travelling ionospheric disturbances (TID) in the F-region made by Heisler (1963) at the Radio Research Laboratories, University of Sydney, Australia, reveals that small perturbations travel with slower apparent speeds than large perturbation and possess a dominant East-West component of movement. Their North-South movement is very small. By contrast large perturbations have a dominant North-South Seasonal component. The difference may not be related entirely to perturbation size but could be the result of ambiguities and limitations in observational techniques. It was suggested that the estimated speed of a perturbation could be a phase speed, group speed or combination of both.

The large perturbations constitute a major ionospheric effect. They are quite prevalent particularly during day light-hours, and in winter months cause almost continuous changes in values of f_oF2 (critical frequency of F2 layer). Their movement is primarily horizontal, and the associated vertical

component of progression which is always observed is almost certainly due to a forward tilt in the wavefront of the disturbance.

It seems probable that there are two components of motion of perturbations in the F-region, an irregular North-South seasonal component which is superimposed on a steady East-West drift of ionization which changes diurnally. There is considerable evidence to suggest that the latter is probably due to North-South electrostatic fields transferred from the dynamo current foci. North-South component of ionization in F region is constrained by the earth's magnetic field and can only take place along the field lines, except by application of an external electrostatic field. The observed phase and group velocities suggest a wave structure and speed of propagation, through medium, of 160 m/s.

The large ionospheric irregularities generally occur in series of three or more of similar size and shape. This suggests that they are caused by a wave of disturbance propagated through ionosphere, with a wavelength of about 100 Km. This was related to the travelling disturbance observed by Munro (1950,1958), which had a spatial length of a few hundred kilometers and were attributed to the travelling pressure waves in the ionosphere.

Chapter 3

PHASE PATH CHARACTERISTICS FOR OBLIQUE RAY PATHS

3.1 Introduction

Phase path is a key parameter in theoretical discussions of a number of practical problems, particularly those involving Doppler frequency shifts produced by relative motion between sender and receiver or by changes in the ionosphere arising, for example, from Travelling Ionospheric Disturbances. For a typical HF oblique ray path from a transmitter T to a point of reception R it is possible to calculate the length, P, of phase path. For a specified ionospheric electron density model P can be found by numerical integration in a suitable computer ray tracing program or, for some simple models, by evaluation of an appropriate analytical expression.

3.2 Relation between Phase Path Length and Ground Range[5]

Phase path (P) is a function of frequency (f) and elevation angle (Δ) and can be written as

$$P = P(f, \Delta) \qquad (3.1)$$

It is assumed that the ground range D between transmitter and receiver remains constant. When the frequency is changed by df, the angle of arrival Δ ,

measured from the horizontal, must therefore change by an amount d Δ to correspond to the new ray path.

Total differential of relation (3.1) can be written as

$$\frac{dP}{df} = \frac{\partial P}{\partial f} + \frac{\partial P}{\partial \Delta} \frac{d\Delta}{df} \tag{3.2}$$

The total change in phase path for a given change in frequency is given by equation (3.2) subject to the condition that $\frac{dD}{df}$ is zero (where D is the ground range). Since D is also a function of frequency and elevation angle, we can write, similarly

$$\frac{dD}{df} = \frac{\partial D}{\partial f} + \frac{\partial D}{\partial \Delta} \frac{d\Delta}{df} \tag{3.3}$$

this gives

$$\frac{d\Delta}{df} = -\frac{\partial D}{\partial f} \Big/ \frac{\partial D}{\partial \Delta}$$

We then have

$$\frac{dP}{df} = \frac{\partial P}{\partial f} - \frac{\partial D}{\partial f}\left(\frac{\partial P}{\partial \Delta} \Big/ \frac{\partial D}{\partial \Delta}\right) \tag{3.4}$$

using equations (2.8a), (2.8b) and (2.8c), we get

$$P - D\cos\Delta = 2\int_{R_o}^{r_v} \frac{1}{r}(\mu^2 r^2 - R_o^2 \cos^2\Delta)^{\frac{1}{2}}\, dr \tag{3.5}$$

Partial differentiation of equation (3.5) with respect to elevation angle, gives

$$\frac{\partial P}{\partial \Delta} - \cos\Delta \frac{\partial D}{\partial \Delta} + D\sin\Delta = 2\frac{\partial}{\partial \Delta}\int_{R_o}^{r_v} \frac{1}{r}(\mu^2 r^2 - R_o^2 \cos^2\Delta)^{\frac{1}{2}}\, dr$$

Here both the integrand and the upper limit of the integral are functions of Δ and therefore the differentiation must be carried out according to standard rule, i.e., that if

$$f(y) = \int_{a(y)}^{b(y)} F(x,y)\, dx$$

then

$$\frac{\partial f(y)}{\partial y} = \int_{a(y)}^{b(y)} \frac{\partial F(x,y)}{\partial y}\, dx - F(a,y)\frac{da}{dy} + F(b,y)\frac{db}{dy}$$

In our problem, we have $\frac{da}{dy} = 0$ since the lower limit is constant, and $F(b,y) = 0$ because $\mu r_v = R_o \cos\Delta$ at the apex. Hence

$$\frac{\partial P}{\partial \Delta} - \cos\Delta \frac{\partial D}{\partial \Delta} + D \sin\Delta = 2 \int_{R_o}^{r_v} \frac{\partial}{\partial \Delta}\left[\frac{1}{r}(\mu^2 r^2 - R_o^2 \cos^2\Delta)^{\frac{1}{2}}\right] dr$$

$$= 2 \int_{R_o}^{r_v} \frac{R_o^2 \cos\Delta \sin\Delta\, dr}{r(\mu^2 r^2 - R_o^2 \cos^2\Delta)^{\frac{1}{2}}}$$

$$= D \sin\Delta$$

and therefore, we have

$$\frac{\partial P}{\partial \Delta} = \cos\Delta \frac{\partial D}{\partial \Delta} \qquad (3.6)$$

For a fixed frequency the ground range D and phase path P are related through the elevation angle as shown in equation (3.6) above. The slope of the plot for a fixed frequency f, with D as abscissa and

P as ordinate, is $\cos\Delta$. This is true for any profile.

If 'f' is less than or equal to the vertical critical frequency f_c, P tends to twice the phase height as elevation angle approaches 90 deg and ground range approaches zero. The tangent to the curve is horizontal at D = 0. If $f > f_c$, there is a minimum value of ground range (the skip distance) at which, from equation (3.6), P is also minimum.

3.3 Relation between Phase Path Length and Group Path Length [5]

From equations (3.4) and (3.6), we get

$$\frac{dP}{df} = \frac{\partial P}{\partial f} - \cos\Delta \frac{\partial D}{\partial f} \qquad (3.7)$$

Partial differentiation of equation (3.5) w.r.t. 'f', holding similar arguments to those in paragraph 2, gives

$$\frac{\partial P}{\partial f} - \cos\Delta \frac{\partial D}{\partial f} = 2 \int_{R_o}^{r_v} \frac{\partial}{\partial f}\left[\frac{1}{r}(\mu^2 r^2 - R_o^2 \cos^2\Delta)^{\frac{1}{2}}\right] dr$$

Assuming that the ionosphere is spherically stratified about the centre of the earth, i.e. that the electron density is a function of only r, the distance from the center of the earth, and neglecting earth's magnetic field and electron collisions, the

refractive index at distance r from the center of the earth can be written as

$$\mu = [1 - \frac{f_N^2(r)}{f^2}]^{\frac{1}{2}}$$

Hence

$$\mu \frac{d\mu}{df} = \frac{(1 - \mu^2)}{f}$$

Therefore,

$$\frac{\partial P}{\partial f} - \cos\Delta \frac{\partial D}{\partial f} = \frac{2}{f} \int_{R_o}^{r_v} \frac{r(1 - \mu^2)\, dr}{(\mu^2 r^2 - R_o^2 \cos^2\Delta)^{\frac{1}{2}}} \qquad (3.7a)$$

Using equations (2.8a), (2.8b), (3.7), and (3.7a), we get

$$\frac{dP}{df} = \frac{1}{f}(P' - P) \qquad (3.8)$$

Above relation holds good for any profile.

For propagation via the ionosphere P' is always greater than the geometrical path length s between transmitter and receiver whereas P is less than s. Hence from (3.8) the slope of the curve is everywhere positive. There will be cusps in the curve wherever $\frac{dP'}{df}$ becomes infinite. Since $\frac{dP}{df}$ becomes very large as P' becomes very large, a vertical line through f_c must be tangential to the (P,f) curve; this result applies for any ground range.

3.4 Relation between Group Path Length and Ground Range[4]

For a plane earth and horizontally stratified ionosphere, Breit and Tuve's theorem gives the relation between the effective (group) oblique-path length P' travelled by a radio-wave packet and the corresponding ground range D as

$$P' = D \sec \Delta$$

$$\text{or} \quad D = P' \cos \Delta \tag{3.9}$$

where Δ is the angle of elevation of the ray path relative to the ground. Provided that the electron density within the layer is a function of height only and that there is no imposed magnetic field, this relation is rigorously true for any electron density profile.

With a curved earth the relation between P' and D is no longer independent of profile and the simple form of the foregoing equation cannot be used. It is possible to place close limits on any one of the quantities P', D and Δ when the other two are known, under the same assumption that the earth's magnetic field is neglected. We assume the equivalent of horizontal stratification, that is, that the electron density is a function of r only, where r is the radial distance from the earth's center.

For the sake of definiteness, we consider the limits that can be put on P', given D and Δ. Consider the ray path geometry of Figure 3.1 where the parts of the path below ionosphere, denoted by a subscript 2, are related by the rigorous equation[4]

$$P_2' = 2R_o \sin(D_2/2R_o) \sec(\Delta + D_2/2R_o)$$

The limits on P_1', the effective (group) path within the ionosphere, are obtained as follows.

$$P_1' = \int \mu' \, ds = \int \frac{ds}{\mu}$$

Also

$$\frac{ds}{\mu} = \frac{r \, d\theta}{\mu \sin i}$$

Therefore

$$P_1' = \int \frac{R_o \, r^2 \, d\theta}{R_o(R_o + h_o) \sin i_o}$$

since

$$r \sin i = (R_o + h_o) \sin i_o$$

All the above integrals are taken over the path within the layer. Now suppose that we can put definite limits on r within the layer, such that

$$r_{min} \leq r \leq r_{max}$$

It follows that

$$\frac{r_{min}^2 \, D_1}{R_o(R_o + h_o) \sin i_o} \leq P_1' \leq \frac{r_{max}^2 \, D_1}{R_o(R_o + h_o) \sin i_o}$$

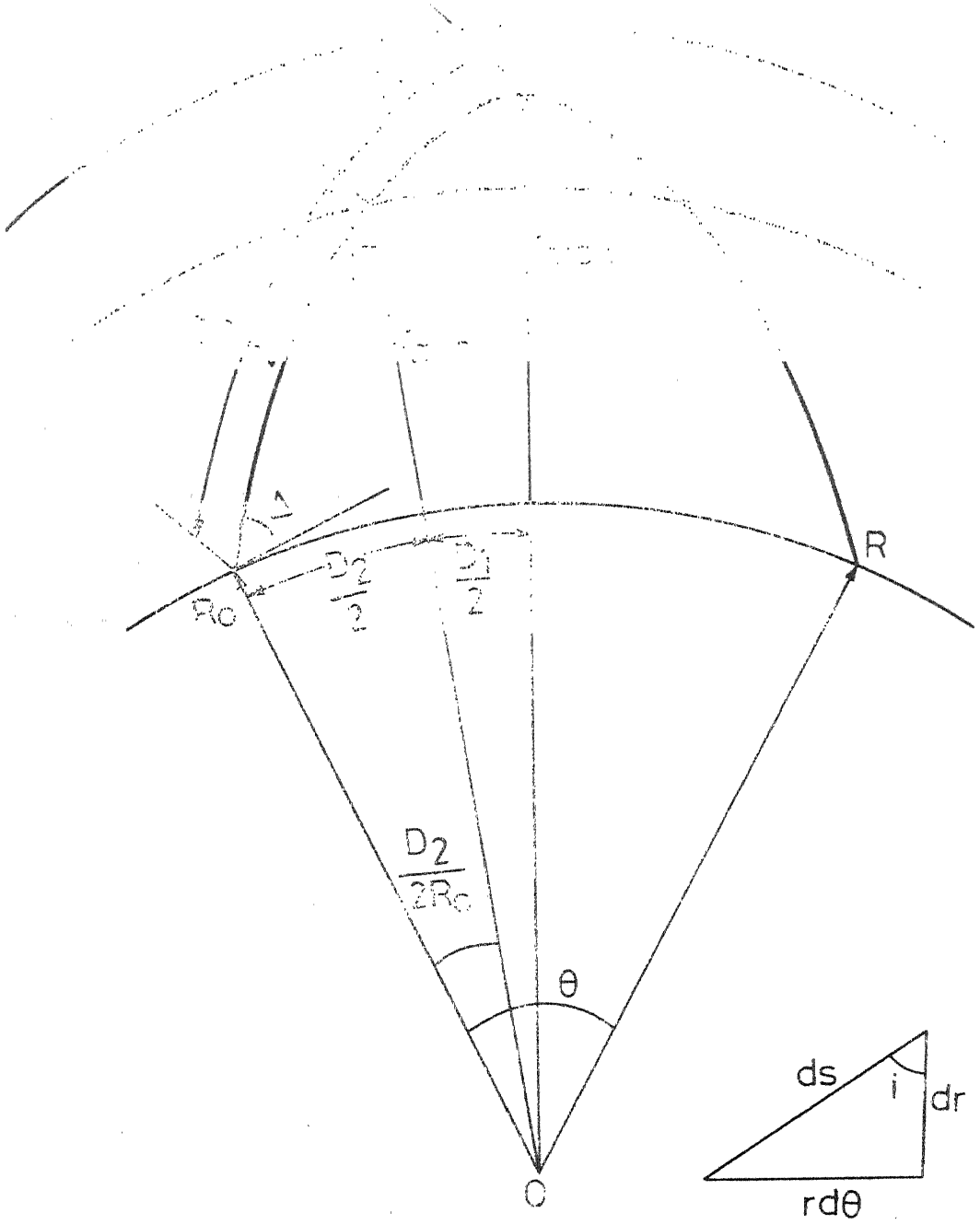

Fig. 3.1

since $R_o \cos\Delta = (R_o + h_o) \sin i_o$

we have, finally

$$\frac{r_{min}^2}{R_o^2} D_1 \sec\Delta \leq P_1' \leq \frac{r_{max}^2}{R_o^2} D_1 \sec\Delta \qquad (3.10)$$

Thus Breit and Tuve's theorem may be written in the form

$$P_1' = \alpha D_1 \sec\Delta \qquad (3.11)$$

where $\alpha = 1$ for a plane earth and slightly greater than 1 for a curved earth.

If we assume that the base of ionosphere extends down to the earth then

$$\frac{r_{min}^2}{R_o^2} = 1$$

and

$$\frac{r_{max}^2}{R_o^2} = \frac{(R_o + h_m)^2}{R_o^2}$$

where h_m is the height of maximum ionization, and thus limits on P_1' in an inequality (3.10) reduces to

$$D \leq P' \cos\Delta \leq \frac{(R_o + h_m)^2}{R_o^2} D \qquad (3.11)$$

For a path involving reflection at the ionsphere, P cannot be less than $2h_o$, where h_o is the height of the base of the ionosphere, but is less than s.

For a finite ground range P is therefore always finite, and must approach some finite limiting value P_c for the penetration condition at which P' becomes infinite. An infinite value of P' for a finite value of D can occur only at $\Delta = 90^\circ$, as may be seen from the conditions (3.11) which apply for any profile. From equations (2.8a) and (2.8c), we get

$$P - D \cos \Delta = 2 \int_{R_o}^{r_v} \frac{(\mu^2 r^2 - R_o^2 \cos^2 \Delta)^{\frac{1}{2}}}{r} dr$$

Hence, when $\Delta = 90^\circ$

$$P_c = \lim_{r_v \to (R_o + h_m)} [2 \int_{R_o}^{r_v} \mu \, dr] = 2h_c$$

where h_c is the limiting value of phase height, i.e., the phase height for $f = f_c$. The value of P_c is therefore independent of the ground range.

Chapter 4

ANALYSIS TECHNIQUE

The effect of elevation angle and frequency on HF radio transmission through a regular as well as perturbed ionosphere may be accurately and conveniently simulated through the use of digital ray tracing techniques in which the effect of electron density variations (provided they are sufficiently slow for ray theory to hold), magnetic field changes and electron collisions are taken into account. A three dimensional ray tracing computer program based upon work by Jones (1966) has been used in this thesis work. The program utilizes the ray tracing differential equations developed by Haselgrove (1954) and the Appleton-Hartree equation for the index of refraction in the ionosphere. In addition to determining the three dimensional ray path, program was also used to determine the effects of ionospheric irregularities upon the ray path trajectories, ground range, phase path, group path etc. Phase path characteristics for oblique ray path have also been studied.

4.1 Ray Tracing Relationships

The path followed by a radio wave through an inhomogeneous medium, such as the ionosphere, is

described by a set of differential equations relating the coordinates of a point on the ray path. Haselgrove has derived these differential equations (for a general coordinate system) from Hamiltonian optics using Fermats principle of stationary time.

Fermat principle states that a ray travels between two points along a path such that the time taken is minimized. This principle is stated in the notation of the calculus of variations as:

$$\delta \int M \, ds = 0 \qquad (4.1)$$

where M = the ray refractive index

$= \mu \cos \alpha$

μ = the phase refractive index

α = the angle between wave normal and wave direction

ds = an element of path length along the ray path.

Applying Euler's variational principle to equation (4.1) expressions for the curvature of the ray may be obtained in terms of M and its derivatives with respect to position and direction. But M can be found only when the wave normal direction is known; hence the latter must be included as an extra set of variables. However, these equations for

the curvature of the ray may be transformed into ones which give the rate of change of wave normal direction in terms of the phase refractive index and its gradients. The ray refractive index and ray direction are thus eliminated from the ray tracing equations.

The Haselgrove equations in spherical coordinates r, θ, and φ are :

$$\frac{dr}{dt} = \frac{1}{\mu\,\mu'}\left[V_r - \frac{\mu\,\partial\mu}{\partial V_r}\right]$$

$$\frac{d\theta}{dt} = \frac{1}{\mu\,\mu'\,r}\left[V_\theta - \frac{\mu\,\partial\mu}{\partial V_\theta}\right]$$

$$\frac{d\varphi}{dt} = \frac{1}{\mu\,\mu' r\sin\theta}\left[V_\varphi - \frac{\mu\partial\,\mu}{\partial V_\varphi}\right] \qquad (5.2)$$

$$\frac{dV_r}{dt} = \frac{1}{\mu'}\,\frac{\partial\mu}{\partial r} + V_\theta\,\frac{d\theta}{dt} + V_\varphi \sin\theta\,\frac{d\varphi}{dt}$$

$$\frac{dV_\theta}{dt} = \frac{1}{r}\left[\frac{1}{\mu'}\,\frac{\partial\mu}{\partial\theta} - V_\theta\frac{dr}{dt} + r\,V_\varphi\cos\theta\frac{d\varphi}{dt}\right]$$

$$\frac{dV_\varphi}{dt} = \frac{1}{r\sin\theta}\left[\frac{1}{\mu'}\,\frac{\partial\mu}{\partial\varphi} - V_\varphi\sin\theta\,\frac{dr}{dt} - r\,V_\varphi\cos\theta\,\frac{d\theta}{dt}\right]$$

where

μ = real part of the phase refractive index of the medium

μ' = real part of the group refractive index of the medium

$\mu' = \mu + f \frac{\partial \mu}{\partial f}$

$\bar{V}$ = a vector, directed normal to the phase front of the ray, of magnitude μ with V_r, V_θ and V_φ, its components in the r, θ and φ direction, respectively

t = group path length (the independent variable)

f = frequency.

The set of first-order partial differential equations are solved numerically to give the locus of the ray as it traverses the medium which is characterized by its parameters such as phase refractive index and group refractive index. The ray tracing procedure is started with initial conditions (i.e., height of transmitter, azimuth angle of transmission, and elevation angle of transmission) and subsequently the differential equations are solved numerically using an Adams-Moulton method with Runge-Kutta starter.

In addition to the six basic equations necessary to calculate the ray path, the program also simultaneously integrates several other

differential equations that are used to determine the Doppler frequency shift, and the absorption that the radio wave experiences as it propagates through the ionosphere. The relationships used to determine these parameters are given in Sections 4.6 and 4.7 respectively.

4.1.1 Refractive Index of the Ionosphere[2]:

Prediction of ionospheric effects upon radio waves requires the knowledge of the complex phase and group refractive index of the medium. Since

$$\eta' = \eta + f \frac{\partial \eta}{\partial f} \qquad (4.3)$$

both η and η' are known if η is available as a function of frequency.

In the presence of the earth's magnetic field and electron collisions, the complex phase refractive index of the ionosphere is given by the Appleton-Hartree equation

$$\eta^2 = (\mu - i\chi_i)^2$$

$$= 1 - \frac{X}{1 - iZ - \frac{Y_T^2}{2(1-X-iZ)} \pm \sqrt{\left(\frac{Y_T^4}{4(1-X-iZ)^2} + Y_L^2\right)}} \qquad (4.4)$$

where

μ = real part of the phase refractive index

χ_i = imaginary part of the phase refractive index

$Z = \nu / \omega$

$$X = \omega_N^2 / \omega^2 = \frac{f_N^2}{f^2} = \frac{Ne^2}{m \varepsilon_o \omega^2}$$

$$Y = \omega_H / \omega = eB/m\omega$$

$$Y_L = Y \cos\theta = e B_T / m \omega$$

$$Y_T = Y \sin\theta = eB_L / m \omega$$

ν = collision frequency of electrons

f_N = plasma frequency

f = operating frequency

ω = angular frequency

e = charge of an electron (1.59×10^{-19} coulombs)

B = magnetic induction vector

m = mass of an electron (9.11×10^{-31} Kg)

N = number density of free electrons

ε_o = electric permittivity of free space (8.854×10^{-12} F/m)

θ = angle between wave normal and geomagnetic field.

In the absence of electron collision

$$\eta^2 = 1 - \frac{2X(1-X)}{2(1-X) - Y_T^2 \pm \sqrt{(Y_T^4 + 4Y_L^2(1-X)^2)}} \qquad (4.5)$$

In the absence of magnetic field

$$\eta^2 = 1 - \frac{X}{1-iZ} \qquad (4.6)$$

Neglecting both the magnetic field and electron collisions:

$$\eta^2 = 1-X = 1 - \frac{81N(h)}{f^2} \qquad (4.7)$$

where N is electron density as a function of height.

4.1.2 Ionospheric Electron Density Model[9,10] :

An analytical model, which represents the general features of the equatorial ionosphere (afternoon, equinox, sunspot maximum) was used to represent electron density contours. The model is an alpha Chapman layer with parameters which vary with geomagnetic latitude. It is represented by

$$f_N^2 = f_c^2 \, e^{\frac{1}{2}(1-Z-e^{-Z})} \qquad (4.8)$$

where $Z = (h - h_{max}) / H$

f_N = the plasma frequency in MHz

f_c = the critical frequency in MHz

h_{max} = the height of maximum electron density in Km

H = the scale height in Km.

f_c, h_{max} and H vary with the geomagnetic latitude in the following ways:

$$f_c = 15 \text{ MHz} \quad \text{for } h < 100 \text{ Km}$$

$$f_c = \sqrt{(50(\lambda/8)^2 \exp(2-|\lambda/8|) + 40)} \quad \text{for } h \geq 100 \text{Km}$$

$$h_{max} = 350 \text{ Km} \quad \text{for } h < 100 \text{ km or } \lambda \geq 24^\circ$$

$$h_{max} = 430 + 80 \cos\left(\frac{180}{24}\lambda\right) \quad \text{for } h \geq 100 \text{ Km and } \lambda < 24^\circ$$

H is determined by the constraint that $f_N = 2$ MHz at h = 100 Km

λ is the geomagnetic latitude in degrees.

The profiles of ionospheric electron density model (BULGE) for four different latitudes are illustrated in Figure 4.1.

4.1.3 Electron Density Perturbation Model[9,10]:

The following model was used to represent the ionospheric electron density perturbation. It is an east-west toroidal irregularity with an elliptical cross section

$$N = N_o[1 + \Delta(r,\theta)] \qquad (4.9)$$

where

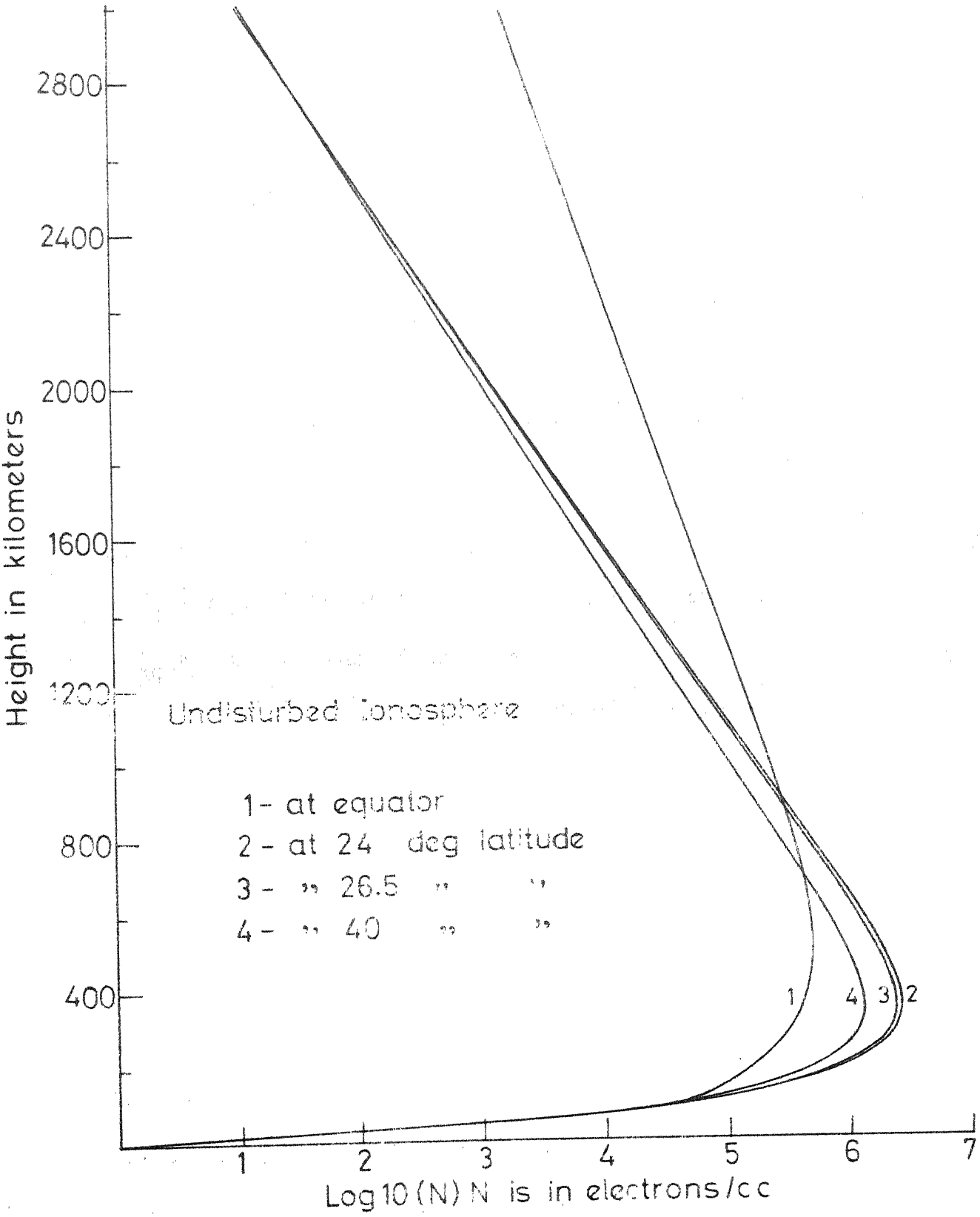

Fig.4.1 Bulge profile for different latitude

N = electron density of the ionosphere including the effects of the torus

N_o = electron density of the ionosphere neglecting torus effect (specified by any electron density model)

$$\Delta(r,\theta) = Co \exp\left[-\left(\frac{(R_o+H_o)(\theta-\pi/2+\lambda)\cos\beta+(R-R_o-H_o)\sin\beta}{A}\right)^2 - \left(\frac{(R-R_o-H_o)\cos\beta-(R_o+H_o)(\theta-\pi/2+\lambda)\sin\beta}{B}\right)^2\right] \quad (4.10)$$

where

C_o = amplitude of the perturbation at the center

R_o = the radius of the earth

R, θ, φ = position in geomagnetic spherical polar coordinates

A = the semimajor axis of the ellipse in Km

B = the semiminor axis of the ellipse in Km

β = the tilt of an ellipse

H_o = the height of the torus above ground

λ = geomagnetic latitude of torus.

Throughout the remainder of this thesis, the electron density perturbation will be referred to as the Torus.

4.1.4 Model of the Earth's Magnetic Field[2] :

The earth's magnetic field was represented by an earth centered dipole model. This is determined

from the following mathematical relationships:

$$|H| = H_o\left(\frac{R_o}{R_o+h}\right)^3 (1 + 3\cos^2\theta)^{\frac{1}{2}} \qquad (4.11)$$

$$\delta = \tan^{-1}(2\cot\theta) \qquad (4.12)$$

where

$|H|$ = magnitude of earth's magnetic field

H_o = surface magnitude of earth's magnetic field at equator

h = height above ground

R_o = Radius of earth

θ = geomagnetic colatitude

δ = magnetic dip angle

4.2 Doppler Frequency Shift

A radio wave propagating through a medium whose index of refraction is changing with time experiences a Doppler frequency shift. The instantaneous frequency shift Δf, in cycles per second, is given by the time derivative of the phase shift :

$$\Delta f = \frac{d}{dT}(\Delta\varphi/2\pi) \qquad (4.13)$$

The phase shift is obtained from

$$\Delta\varphi = 2\pi \frac{f}{c}\Delta P \qquad (4.14)$$

where ΔP is the change in the phase path. Equations (4.13) and (4.14) together give

$$\Delta f = - \frac{f}{c} \frac{d}{dT}(\Delta P) \qquad (4.15)$$

the negative sign indicates that a decrease in phase path produces a positive frequency shift and vice versa. From Davies (1968)

$$\frac{d(\Delta P)}{dT} = \frac{dP}{dT} = \frac{d}{dT} \int_s \mu \, ds = \oint_s \frac{\partial \mu}{\partial T} ds \qquad (4.16)$$

where s is the ray path, and μ is the real part of the phase refractive index.

Substituting (4.16) into (4.15), we have

$$\Delta f = - \frac{f}{c} \int_s \frac{\partial \mu}{\partial T} ds \qquad (4.17)$$

Neglecting the earth's magnetic field and electron collisions, we have

$$\frac{\partial \mu}{\partial T} = \frac{\partial}{\partial T}(1 - X)^{\frac{1}{2}}$$

$$= - \frac{\partial X}{\partial T}\left(\frac{1}{2\mu}\right) = -(K/2\mu f^2) \frac{\partial N}{\partial T} \qquad (4.18)$$

where K is a constant equal to 80.5×10^6. The expression for Δf may thus be written as

$$\Delta f = \frac{K}{2\mu f} \int_s \frac{\partial N}{\partial T} ds \qquad (4.19)$$

As discussed in Section 2.3.4) the torus is thought to move in a North-South direction with an average

velocity of 160 m/sec. Taking this into account and using equation (4.9), $\frac{dN}{dT}$ may be conveniently derived from

$$\frac{dN}{dT} = \frac{dN}{d\lambda} \frac{d\lambda}{dx} \frac{dx}{dT} \tag{4.20}$$

where x is the longitudinal displacement of the torus relative to the geomagnetic pole, and λ is the geomagnetic latitude of the center of the torus.

Since $\frac{d\lambda}{dx}$ equals $-\frac{1}{r}$:

$$\frac{dN}{dT} = -\left(\frac{1}{r}\right) \frac{dN}{d\lambda} \frac{dx}{dT} \tag{4.21}$$

but $$N = N_o[1 + \Delta(r,\theta,\varphi)] \tag{4.22}$$

Therefore

$$\frac{dN}{dT} = -\frac{N_o}{r} \frac{d}{d\lambda}(\Delta(r,\theta,\varphi)) \frac{dx}{dT} \tag{4.23}$$

where $\frac{d\Delta}{d\lambda}(r,\theta,\varphi)$ is obtained by differentiating equation (4.10)

$$\frac{d\Delta}{d\lambda}(r,\theta,\varphi) = -2\Delta(r,\theta,\varphi)\,(R_o+H_o)\left(\frac{P\cos\beta}{A^2} - \frac{Y\sin\beta}{B^2}\right) \tag{4.24}$$

where

$$P = \frac{(R_o+H_o)\,(\theta-\pi/2+\lambda)\cos\beta + (R-R_o-H_o)\sin\beta}{A}$$

$$Y = \frac{(R-R_o-H_o)\cos\beta - (\theta-\pi/2+\lambda)\sin\beta}{B}$$

Thus equation (4.19) may be expressed as

$$\Delta f = \frac{k}{2\mu f} \int_s \frac{dx}{dT}\, 2(R_o+H_o)\,\Delta(r,\theta,\varphi)\, \frac{N_o}{r}\left(\frac{P\cos\beta}{A^2} - \frac{Y\sin\beta}{B^2}\right) ds \tag{4.25}$$

since $ds = \frac{dt}{\mu'}$, t is group path (independent variable)

$$\frac{d(\Delta f)}{dt} = \frac{k}{\mu\mu' f} \frac{N_o}{r}(R_o+H_o) \left(\frac{P \cos\beta}{A^2} - \frac{Y \sin\beta}{B^2}\right) \frac{dx}{dT} \Delta(r,\theta,\varphi)$$

or

$$\frac{d(\Delta f)}{dt} = (R_o+H_o)\left(\frac{P \cos\beta}{A^2} - \frac{Y \sin\beta}{B^2}\right) \Delta(r,\theta,\varphi) \frac{k}{\mu\mu' f} \frac{N_o}{r} \frac{dx}{dT} \qquad (4.26)$$

The above equation is in differential form relative to the group path length t. To find Doppler frequency shift induced by the moving torus upon the radio wave, equation (4.26) is integrated simultaneously along the ray path with the Haselgrove equations.

4.3 Radio Wave Absorption

The attenuation of radio waves in the ionosphere results from collision between electrons and other particles. The incremental absorption per unit length (K) is expressed as

$$K = \frac{\omega}{c} \chi_i \, (8.68 \times 10^3) \text{ dB/Km} \qquad (4.27)$$

where χ_i is the imaginary part of the complex phase refractive index, ω is the angular frequency and c is the velocity of light. Neglecting the effect of the earth's magnetic field, χ_i may be written as

$$\chi_i = \frac{1}{2\mu} \frac{X Z}{1 + Z^2} = \frac{e^2}{2\varepsilon_o m \omega \mu} \frac{N \nu}{\omega^2 + \nu^2}$$

$$= \frac{5.3 \times 10^{-6}}{\mu} \frac{N \nu/\omega}{\omega^2 + \nu^2} \qquad (4.28)$$

where the terms appearing in the equation (4.28) are as defined in Section 4.1.1. Therefore:

$$K = \frac{0.046}{\mu} \frac{N\nu}{\omega^2 + \nu^2} \tag{4.29}$$

The total absorption, A, over the ray path, S, is thus evaluated from:

$$A = \int_S \frac{0.046}{\mu} \frac{N\nu}{\omega^2 + \nu^2} ds \tag{4.30}$$

Expressed in differential form relative to the group path length (t), the above equation, which is integrated simultaneously with the ray tracing equations, becomes:

$$\frac{dA}{dt} = \frac{0.046}{\mu\mu' \omega^2 + \nu^2} \frac{N\nu}{} \tag{4.31}$$

4.4 Program Structure

A three dimensional ray tracing program written by Jones (1966, 1968) in FORTRAN language for the CDC 3600 computer and modified by Sarabjit (1972) in FORTRAN IV for an IBM 7044 computer has been used. It has a main program followed by essential subroutines. When using this program the ionospheric models, which define electron density, and the earth's magnetic field as a function of position in space, have been specified. The effect of electron collisions have been neglected. Each of these characteristics of the ionosphere is defined by a separate routine. There are several versions of the subroutine RINDEX. These correspond to inclusion or exclusion of the effects of

earth's magnetic field and collisions. Data required for initialization have been read into an array designated as the W array.

4.4.1 Accuracy of the Program:

The numerical integration subroutine has a built-in mechanism to check errors and adjust the integration step size accordingly. The user specifies the accuracy he wants with W(42). To get a very accurate but expensive ray trace a small W 42 (about 10^{-7} or 10^{-8}) may be used, while for a cheap but approximate trace a large value of W 42 (10^{-3} or even 10^{-2}) is used. W 42 is the maximum allowable relative error in any single step for any of the equations being integrated. For the purpose of this work an accuracy of 10^{-4} has been used.

4.4.2 Coordinate Systems:

The program uses two different spherical polar coordinate systems, namely, a geographic and a computational coordinate system. Input data for the coordinates of the transmitter (W 14 and W 16), and input data for the coordinates of the north pole of the computational coordinate system (W 13 and W 15) are entered in geographic coordinates. If W 13 is equal to 0, W 15 equal to 90^{o}, the two north poles superimpose and the two coordinate systems become the same. When the two coordinate systems do not coincide, the three type of ionospheric models

calculate electron density, the earth's magnetic field, and collision frequency in terms of the computational coordinate system. In this work the dipole model of the earth's magnetic field uses the axis of the computational coordinate system as the axis for the dipole field. When dipole model is used, the computational coordinate system is a geomagnetic coordinate system, and therefore electron density has been defined in geomagnetic coordinates.

Chapter 5

RESULTS

The computerized three dimensional ray tracing program, described previously, has been used to study the ray path trajectories of the radio wave propagating through the ionosphere in HF band of frequencies, effect of torus on the ray path trajectories, phase path/group path variations with elevation angle, and phase path oblique ionograms. The details and results of these predictions are presented in the following sections.

5.1 Ray Path Trajectories

The results have been computed for the radio waves in HF band of frequencies (5.30 MHz) for all elevation angles of transmission, in presence of magnetic field and neglecting the effect of electron collisions. These computed results are given in Table 5.1. (In this table True Path is the path traversed by a radio wave with free space velocity). Both the transmitter as well as receiver are located on ground, transmitter being located at Kanpur (26.5°N, 80° E). The azimuth angle of transmission has been taken as 180° corresponding to the North-South propagation along constant geomagnetic longitude. The ray paths have been plotted using the IBM 1800 computer and associated plotter only for frequency range of

5-20 MHz at step of 5 MHz and for elevation angle 30^{o}-90^{o} at step of 10^{o}. These plots are illustrated in Figures 5.1 through 5.4. The ray paths plotted for the undisturbed case exhibit typical features of ionospheric radio wave propagation, in that :

- the ray paths are symmetrical about the point of reflection
- the height of reflection increases with the increasing elevation angle, consistent with the electron density profile used
- rays propagating vertically upwards are returned directly to the transmitter
- the rays bend towards the region of decreasing electron density; that is: rays bend towards the earth in the bottom half of the layer and away from the earth in the top half of the layer, etc.
- a 20 MHz signal studied for 30-60 degrees at the step of 10 degree elevation angle penetrates through the ionosphere at 60 degree elevation angle. It is observed that the ground range decreases as the elevation angle is increased from 30 degree to 40 degree. The rays which experience this effect are low angle rays. A 50 degree elevation angle ray is reflected back towards the ground at distance longer than the skip distance. This is higher

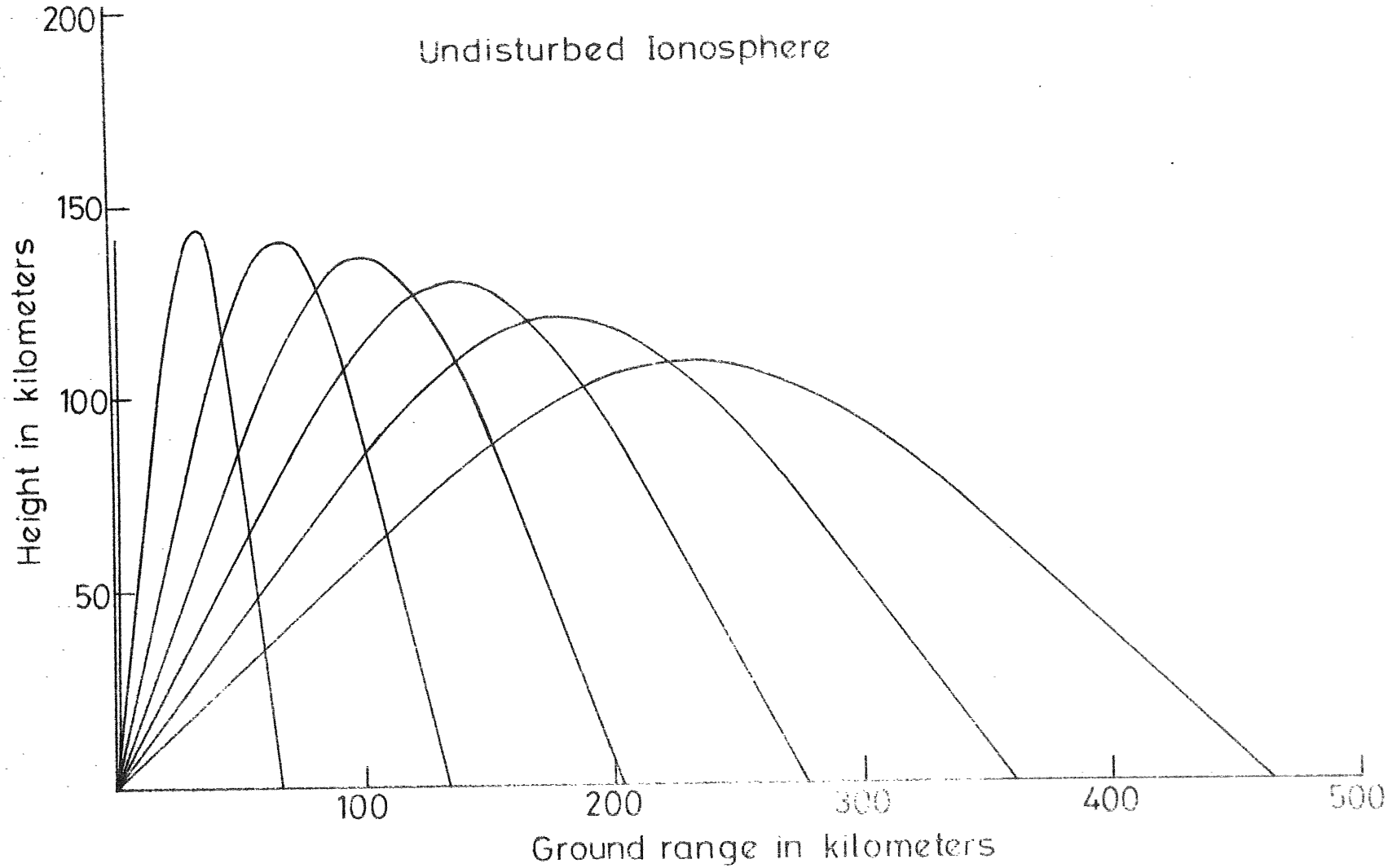

Fig. 5.1 Freq. 5 MHz elevation 30-90 deg.at step 10 deg.

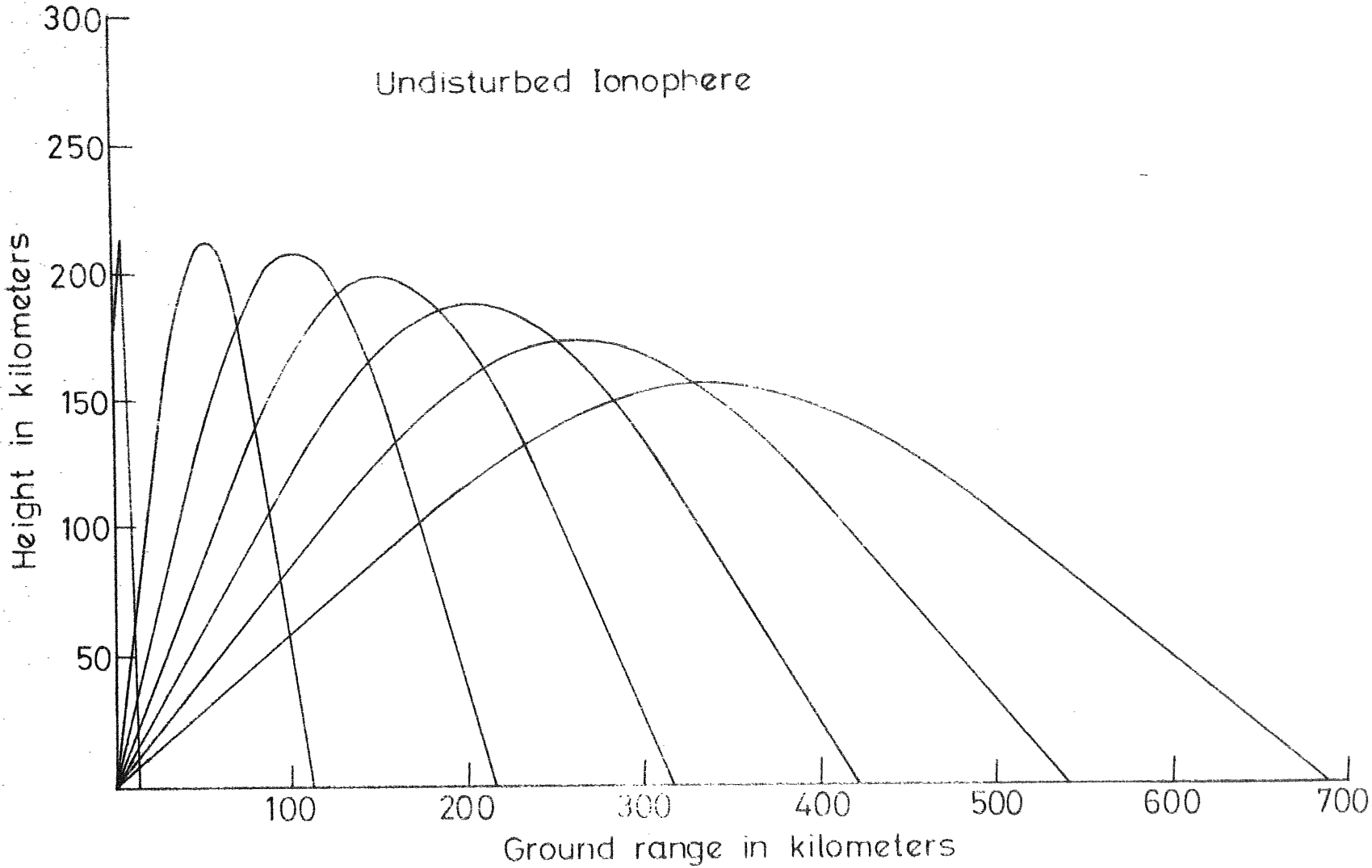

Fig. 5.2 Freq. 10 MHz elevation 30 - 90 deg. at step 10 deg.

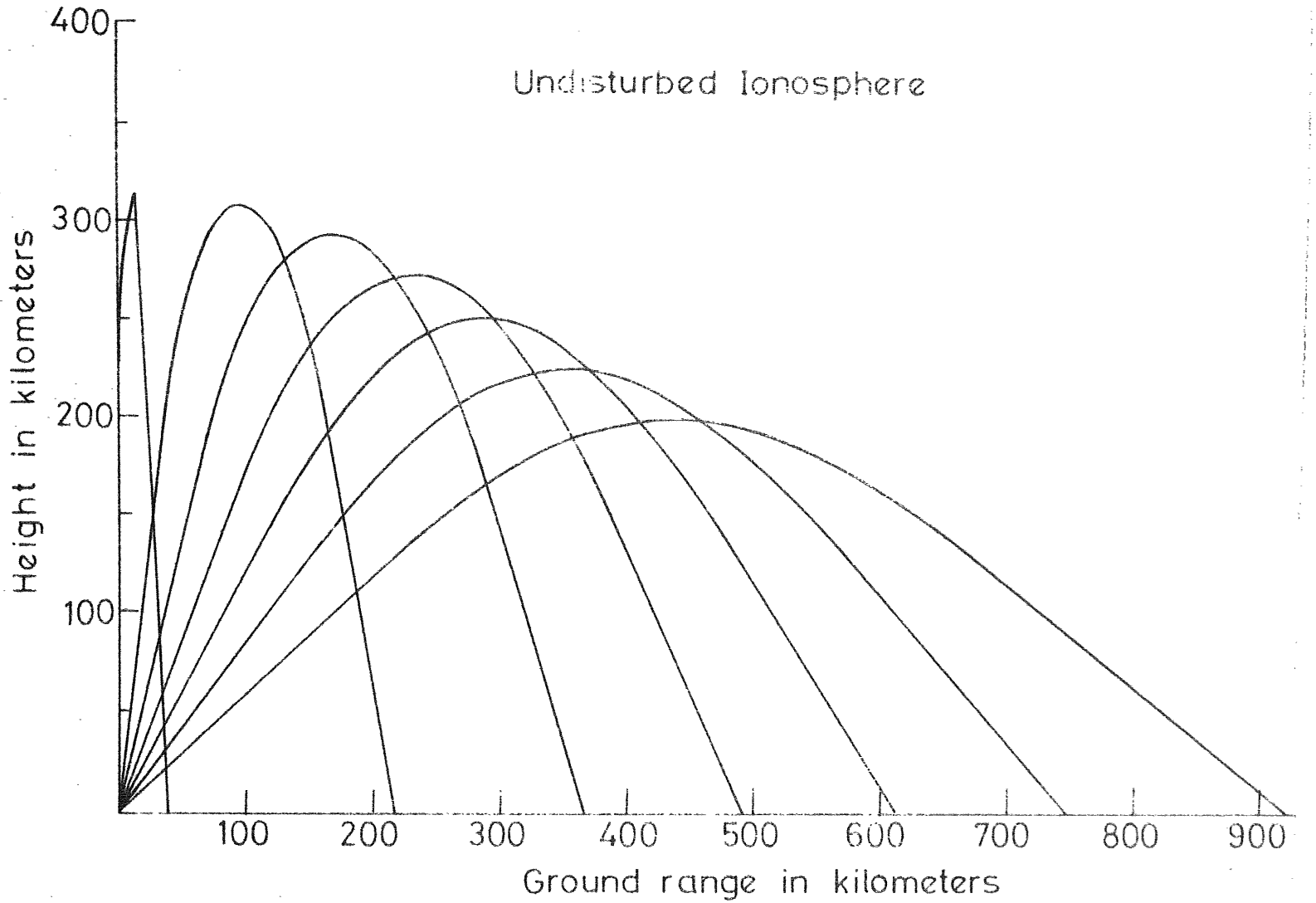

Fig. 5.3 Freq. 15 MHz elevation 30 – 90 deg. at step 10 deg.

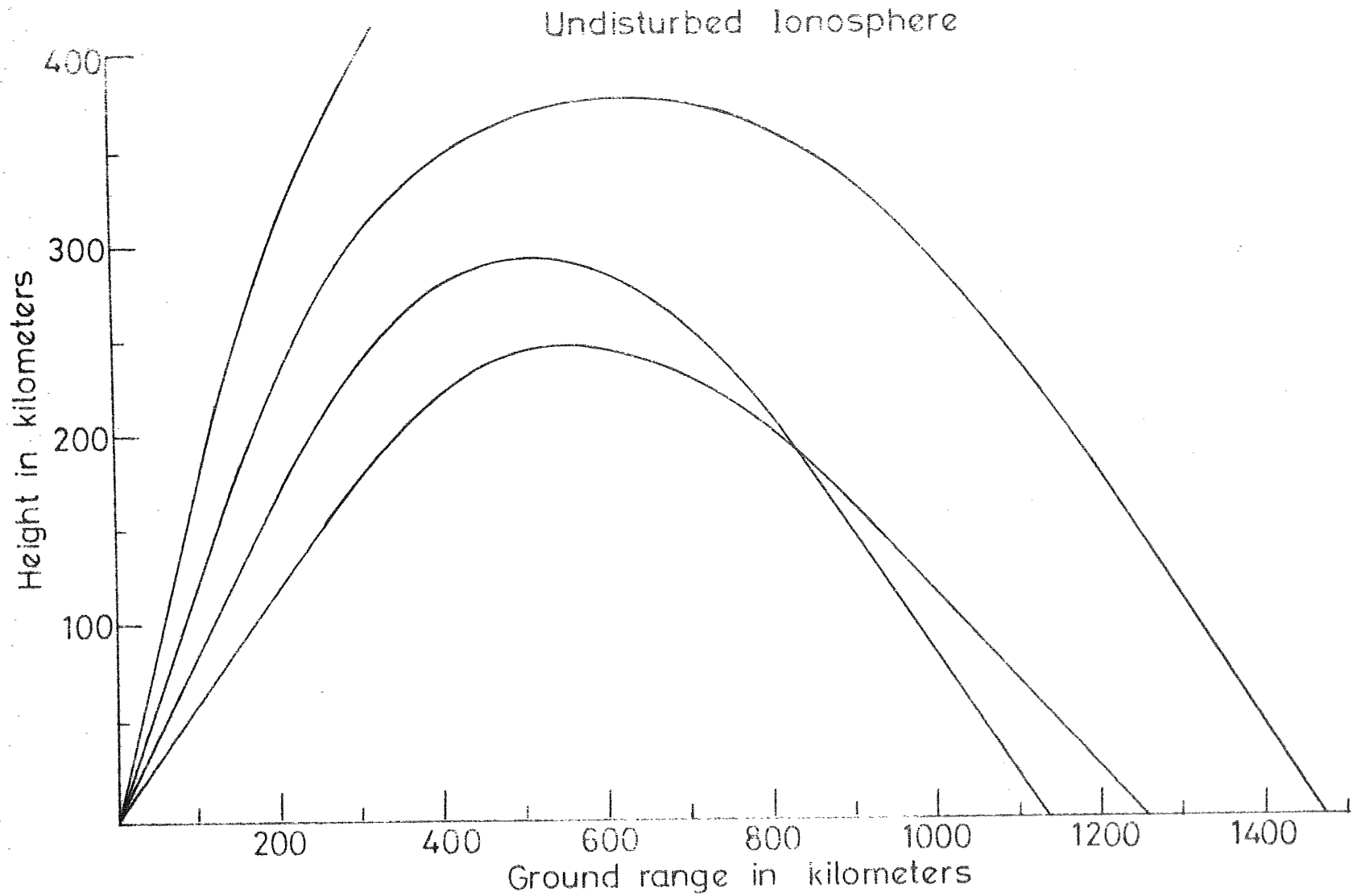

Fig. 5.4 Freq. 20 MHz elevation 30 - 60 deg. at step 10 deg.

angle ray and is known as a pederson ray. For higher angle rays, the ground range increases with increase in the elevation angle. The mechanism of pederson ray runs as given below.

The refractive index decreases as the wave penetrates into the regions of greater electron density (equation (4.7)) and the angle of refraction increases correspondingly (equation (2.6)). It is seen from Bulge profile of Figure 4.1 that dN/dh, the rate of change of electron density with height, decreases until it becomes zero at the height of maximum electron density and beyond this height it becomes negative corresponding to the penetration condition. The rays reflected back towards the ground from the height of maximum ionization experience small bending as dN/dh is very small and return back to the ground at distance larger than the skip distance. These rays are high angle rays and are known as pederson rays.

- the critical frequency at Kanpur is 15.4 MHz.

The radio waves transmitted at frequency higher than 15.4 MHz penetrate through the ionosphere at some elevation angle less than 90°. In these cases there will be both low angle as well as high angle rays.

5.2 Effect of Perturbation on HF and VHF Propagation

To study the effect of torus on HF radio wave a 20 MHz signal has been considered for elevation angle 30-60 Deg at step of 10 Deg. The torus is located in space such that radio wave passes through the center of the torus. The torus to background ionization density has been taken as 1.1. The semimajor and semiminor axes of an ellipse have been taken as 150 Km and 50 Km based on the experimental observations. The torus is tilted down to the South at an angle of 15 degree. Both the transmitter and receiver are located on the ground, transmitter being located at Kanpur (26.5^{o}N, 80^{o}E). To observe the effect on VHF signal, a 41 MHz signal transmission, from satellite located at the height of 1000 Km above ground, has been considered. The receiver in this case is located on ground. The computed results are shown in Table 5.2 and the plots for HF signal are illustrated in Figures 5.5 and 5.6. The effect of the presence of the torus on the radio wave path are listed below.

- Ray path trajectories are significantly affected in the vicinity of the torus, the rays whose wave reversal occur near the center of the torus are the most significantly affected.

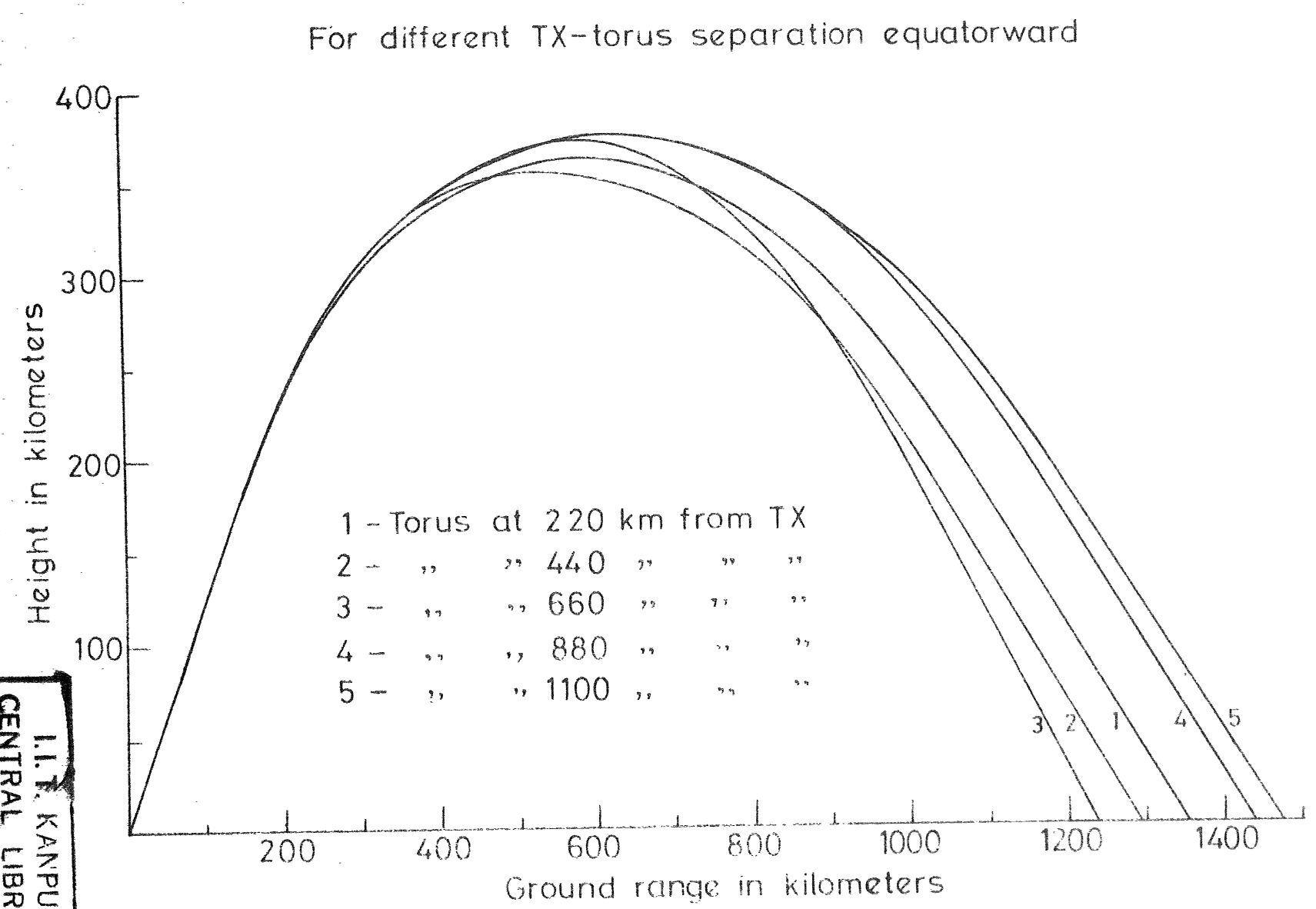

Fig. 5.5 Freq. 20 MHz elevation 50 deg.

For different TX-torus separation equatorward

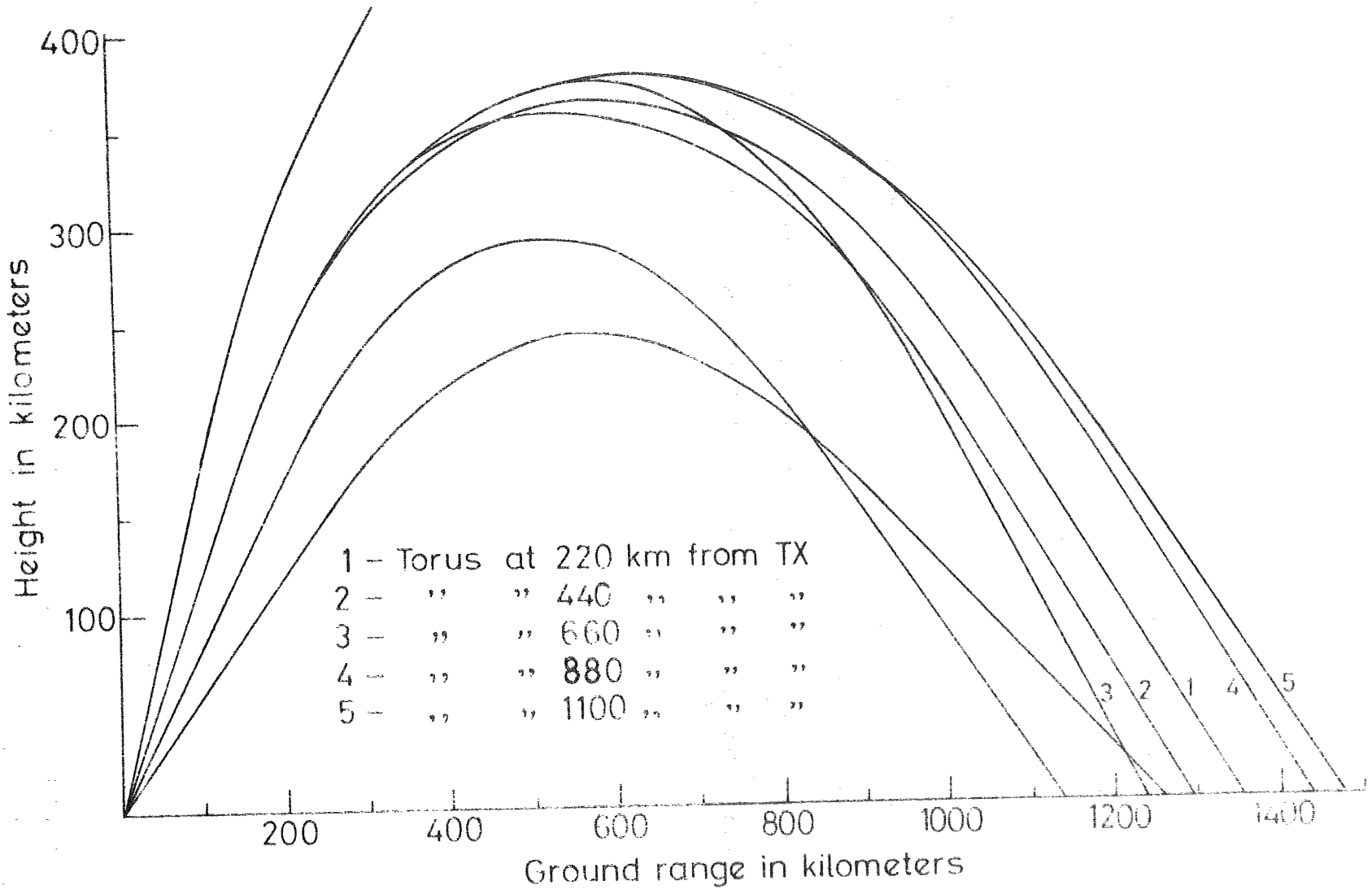

Fig.5.6 Freq. 20 MHz elevation 30-60 deg at step 10 deg.

- The ray path symmetry about the point of reflection is not significantly disturbed for the intensity of perturbation used in this work.
- There is significant change in various path lengths and skip distance. For example, for a 20 MHz ray with an elevation angle of 50^{o}, the phase path and ground range can change by as much as 100 Km depending upon the location of the torus.
- As the torus is moved away from the transmitter towards the point of reflection, where the ray path between ground and the ionosphere experiences the presence of the torus, the various path lengths, ground range and maximum height of reflection of radio wave decreases and this decrease in various parameters is maximum when the torus is located near the point of reflection. If the transmitter torus separation is still increased the radio wave now experiences the presence of the torus along its return path to the ground. The effect of the torus now decreases and finally the radio wave path in the presence of the torus is almost same as an undisturbed path.
- The effect of torus on VHF radio signal transmitted from satellite at 41 MHz is insignificant as can be seen from Table 5.3. (In this table straight line path is the path joining the transmitter and receiver by a straight line and Differential Phase Path is the difference between straight line path and the Phase Path). However, this small change in Phase Path and Straight Line Path is significant in radio astronomy.

5.3 Variation of Phase Path/Group Path with Elevation Angle[6]

In this case the effect of earth's magnetic field as well as collision have been neglected and computed results for phase path, group path, and ground range for various elevation angle and for frequencies below and above critical frequency are shown in Table 5.4. The curves, depicting the effect of elevation angle on phase path/group path and ground range for a fixed frequency below and above critical frequency, have been shown in Figure 5.7 and Figure 5.8. It is observed that

- For 'f' (13 MHz) less than vertical critical frequency f_c (15.4 MHz) phase path (P) tends to twice the phase height as elevation angle approaches 90^o and D approaches zero.
- the tangent to the curve (see Figure 5.7) is horizontal at D equal to zero. For frequency 'f' (18 MHz) there is a minimum value of ground range (the skip distance) at which phase path is also minimum.
- The low angle and high angle branches of the curve meet in a cusp as illustrated in Figure 5.7.
- A plot of effective (group) path P' against ground distance D shows a 'nose' near the skip distance (see Figure 5.8). The behaviour of the (D,P) curve is thus quite different from that of the (D,P') curve.

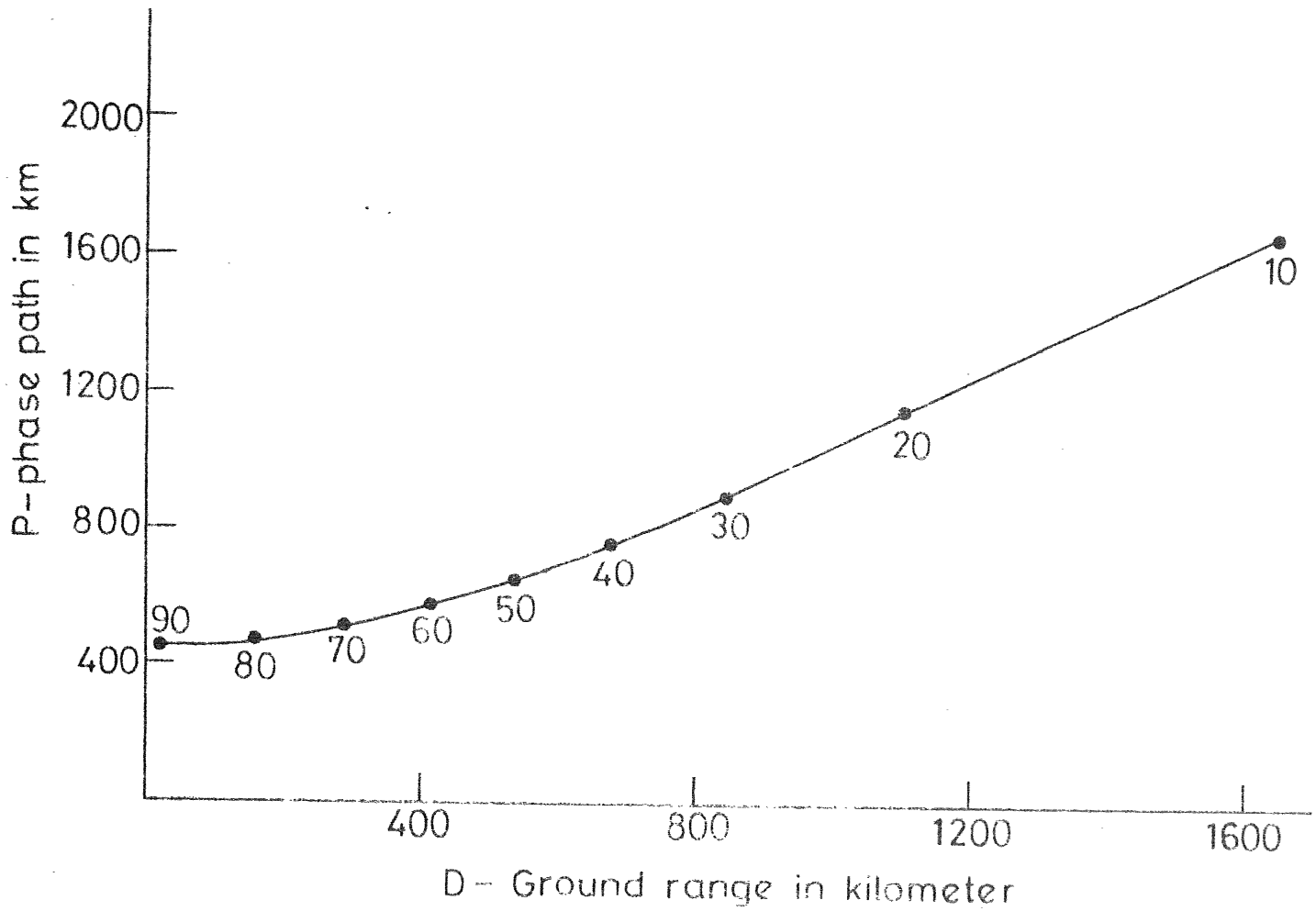

Fig. 5.7 Variation of D and P with elevation angle. Bulge, f=13 MHz, f_c = 15.4 MHz TX at (26.5°N, 80.0°E).

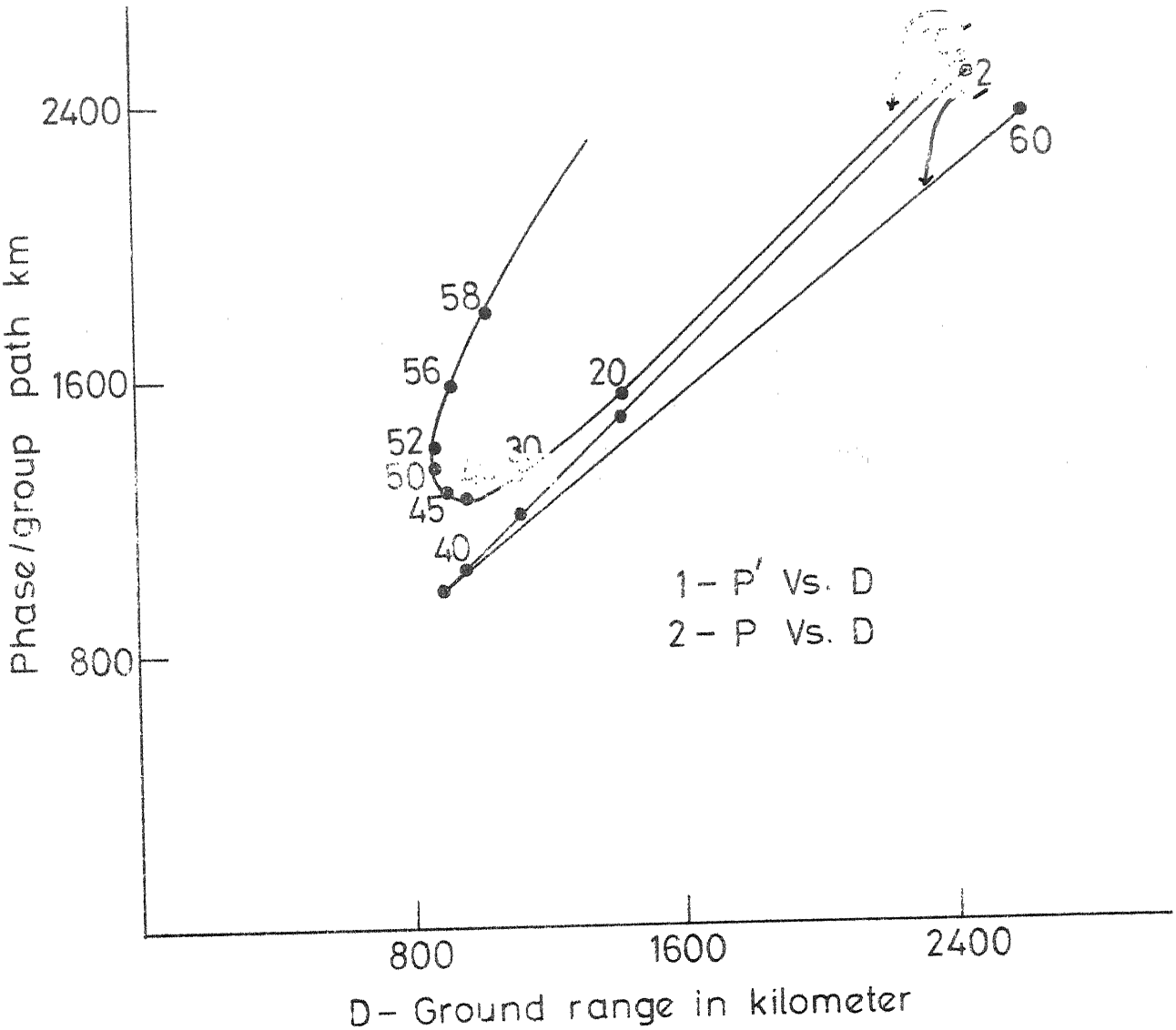

Fig. 5.8 Variation of ground range and phase/group path with elevation angle Bulge, f = 18 MHz, f_c = 15.4 MHz TX at (26.5°N, 80.0°E).

- The slope of (D,P) curve does not undergo any large changes near the cusp, where as the slope of (D,P') curve changes rapidly round the nose.
- These observations are in agreement to those found by Davies(1968) and Gething (1974) for a single parabolic layer.

5.4 Phase Path Oblique Ionogram[6]

For a given ground distance, phase path/group path oblique ionogram is a plot of phase path/group path against frequency for different elevation angle. For frequency of operation below critical frequency there is one set of elevation angle and frequency for which a radio wave is received between two fixed terminal stations, whereas for frequency of operation greater than critical frequency there will two sets of elevation angle and frequency of transmission, for the same communication links. The ray tracing program developed by Jones (1966, 1968) does not incorporate automatic homing technique to select a set of elevation angle and frequency of transmission for a given ground range. However, this may be done by step-by-step method by getting results computed for the nearest Kilometer accuracy in ground range. In this way the user has to pay an exorbitant cost of computation. In view of all these difficulties phase path oblique ionogram could not be completed. The results obtained for some sets of elevation angle and frequency

of transmission for two different ground ranges 500 Km and 250 Km, are given in Table 5.5. While computing these results efforts have been made to select a set of elevation angle and frequency to get computed ground range nearest to the specified value (250 Km and 500 Km) for a given communication link.

TABLE 5.1 COMPUTATION OF GROUND RANGE, PHASE PATH AND GROUP PATH FOR VARIOUS FREQUENCIES AND ELEVATION ANGLES

Elevation Angle Deg.	APOGEE KM	GROUND DISTANCE KM	GROUP PATH KM	PHASE PATH KM	TRUE PATH KM
FREQUENCY = 5 MHz					
0	63.8538	2107.3824	2125.97180	2117.03183	2121.11102
10	78.1343	935.8076	965.67976	949.42618	956.34807
20	94.7220	607.1037	659.43687	631.22401	643.82150
30	109.1143	465.3888	551.60091	502.36491	523.69719
40	120.9260	361.9711	486.35035	417.27026	445.95750
50	129.9931	277.9930	444.82224	357.26733	391.49256
60	136.7102	204.1852	417.86274	314.15034	351.31815
70	141.2751	133.5909	399.74964	283.32249	320.01525
80	143.7139	66.1397	388.96741	264.67869	298.09356
90	144.2311	3.2328	384.49092	258.00597	288.43306
FREQUENCY = 10 MHz					
0	91.9760	2477.9446	2508.23151	2495.08606	2501.36630
10	110.2057	1313.7575	1360.96170	1334.53815	1347.08311
20	135.7307	908.2615	989.20760	941.08337	963.56448
30	156.5410	689.1535	814.73109	739.93250	773.91609
40	173.8873	540.5837	720.73994	615.24419	661.21008
50	188.2905	422.1084	666.24961	528.08496	584.81467
60	199.7578	316.8574	633.82719	463.86781	528.13512
70	207.9897	215.1367	613.84692	416.57449	483.02482
80	212.5782	111.8975	600.87536	385.05031	446.85455
90	213.3033	12.8360	593.30497	371.56338	426.90771

(Continued)

FREQUENCY 15 MHz

0	140.8047	3414.3648	3499.77554	3444.06110	3470.98087
10	143.0990	1814.7361	1883.41554	1843.13948	1862.52307
20	171.7526	1199.9516	1307.17952	1241.26587	1272.48247
30	199.1646	922.9800	1088.70802	983.37553	1031.87770
40	224.9908	748.4447	991.99008	833.55411	903.44699
50	249.7309	613.7998	957.91555	730.99762	825.06342
60	272.9041	492.5008	965.83663	652.96514	771.56580
70	293.8047	367.5669	1006.39594	590.03139	728.49223
80	309.5821	217.9155	1064.44603	538.35811	681.05576
90	314.6039	39.4984	1095.98782	507.40891	632.39747

FREQUENCY 20 MHz

0	256.8679	3310.0286	3486.55981	3363.74738	3422.71115
10	177.0793	2829.9429	2927.12329	2869.42007	2897.38443

MIN.DIS 23.8780 RAY MADE A CLOSEST APPROACH TO REC HT.

20	209.0555	1590.0499	1728.52063	1639.05898	1681.71149
30	247.6866	1261.6192	1480.40762	1326.90823	1389.08121
40	293.8677	1139.09118	1489.24504	1217.35187	1337.93274
50	377.4663	1477.8815	2153.32190	1498.10825	1770.59962
60	413.8076	320.6792	676.25000	445.61528	537.99447

RAY PENETRATES

(Continued)

FEEQUENCY = 25 MHz

0	341.1835	3666.8344	4034.52170	3724.38898	3869.07370
10	220.1012	3882.7427	4063.91681	3951.06064	4006.01123
20	255.3998	2789.0248	2974.68396	2846.97586	2908.17441
30	323.6197	2578.1222	2900.70850	2635.19073	2759.16971
40	455.8933	752.5902	1045.00000	814.95699	917.80948

RAY PENETRATES

FREQUENCY = 30 MHz

0	471.2875	2865.6852	3063.75000	2923.62338	2990.33286

RAY PENETRATES

TABLE 5.2: EFFECT OF PERTURBATION ON GROUND RANGE, PHASE PATH AND GROUP PATH

Frequency 20 MHz

Elevation Angle Deg.	APOGEE KM	GROUND DISTANCE KM	GROUP PATH KM	PHASE PATH KM	TRUE PATH KM
Mag.Field, Extraordinary, No col., No perturbation					
30	247.6866	1261.6192	1480.40762	1326.96823	1398.08121
40	293.9795	1139.0910	1489.24480	1217.35162	1337.93250
50	377.4663	1477.8815	2153.32190	1498.10825	1770.59962
60	413.8076	320.6792	676.25000	445.61528	537.99447
RAY PENETRATES					
No Field, No col., No perturbation					
50	423.5107	3038.6431	3929.72089	2971.42166	3387.24152

Torus-Tx seperation KM	Height of torus above ground KM	APOGEE KM	GROUND DISTANCE KM	GROUP PATH KM	PHASE PATH KM	TRUE PATH KM
Mag.field, No. col., Perturbation 10 percent, Elevation 50 Deg.						
220	250	365.772	1355.120	1985.595	1392.972	1640.192
440	350	357.718	1294.831	1915.536	1338.352	1576.868
660	380	374.507	1239.316	1890.452	1294.672	1539.879
880	330	377.487	1441.000	2126.426	1460.960	1736.718
1100	240	377.466	1477.324	2156.245	1495.650	1770.486
No field, No col., Perturbation 10 percent, 50 Deg.						
660	380	433.943	1906.654	2684.738	1782.139	2166.860

TABLE 5.3: IONOSPHERIC EFFECTS ON SATELLITE SIGNALS

Elevation Angle Deg.	GROUND RANGE KM	Azimuth deviation TX	Azimuth deviation LOCAL	Elevation TX	Elevation LOCAL	GROUP PATH KM	PHASE PATH KM	TRUE PATH KM	STRAIGHT PATH KM	Differential PHASE PATH KM
No field, No col., No perturbation										
300	608.845	-0.053	-0.025	-59.428	55.176	1237.144	1155.681	1195.340	1195.224	39.542
330	4709.341	0.074	0.023	-31.670	-0.000	5189.775	5001.550	5094.122	5053.379	51.829
MINDIS 13.2985 Km										
Mag. Field, Extraordinary, No col., No perturbation										
300	609.568	-0.048	-0.018	-59.400	55.186	1237.807	1155.999	1195.773	1195.649	39.650
330	4765.764	0.072	0.031	-31.901	-0.000	5251.487	5056.702	5151.801	5106.974	50.273
MINDIS 3.2154 KM										
Mag. Field, Extraordinary, No col., Perturbation 10 percent, located at 385 Km from satellite (Tx) equator-ward at height 350 Km above ground										
300	610.503	-0.051	-0.004	-59.364	55.298	1240.443	1154.837	1196.370	1196.200	41.363

TABLE 5.4: DATA FOR PHASE PATH VERSUS GROUND RANGE CHARACTERISTICS

Elevation Angle Deg.	PHASE PATH KM	GROUP PATH KM	GROUND RANGE KM	APOGEE KM
No field, no col. FREQUENCY = 13 MHz				
10	1660.11203	1694.82843	1634.3637	132.5854
20	1137.69321	1195.68356	1099.0154	160.0689
30	897.15826	988.60684	839.3936	185.0800
40	752.74768	886.65970	669.7663	207.5634
50	651.60728	835.86947	535.2146	227.6503
60	574.39824	814.32309	412.6176	245.2708
70	514.53995	809.48001	289.7041	259.1954
80	472.18711	810.70087	160.2658	268.1114
90	451.31850	807.73646	24.7307	270.3928
No field, no col. FREQUENCY = 18 MHz				
10	2446.0233	2480.89893	2530.82797	
20	1440.4379	1487.01300	1566.08089	
30	1126.6123	1191.18713	1322.78902	
40	961.0701	1045.89732	1261.74823	
50	884.1386	984.32897	1352.54863	
60	2536.8380	2374.71051	3712.71152	

TABLE 5.5: DATA FOR PHASE PATH OBLIQUE IONOGRAM

Elevation Angle Deg.	GROUND RANGE KM	PHASE PATH KM	GROUP PATH KM	FREQUENCY MHz
No field, no col.				
10	501.3768	504.63325	512.60515	0.91
20	500.1307	518.43672	539.68216	2.73
30	500.4471	539.83060	589.45547	5.36
40	499.8812	571.41452	664.67851	8.55
50	500.5769	615.05274	783.21387	12.10
60	500.8456	662.14441	979.32755	14.90
70	500.5505	693.20570	1342.77449	16.06
10	250.3083	249.67565	255.63869	0.285
20	249.4446	254.05931	267.43227	0.485
30	250.1973	267.93432	292.05846	0.990
40	250.6223	291.14130	331.54773	2.070
50	249.7085	323.50725	395.69491	3.800
60	249.8515	380.13170	503.01260	6.900
70	249.2546	465.80571	703.61874	11.500
80	250.2635	565.98330	1209.69995	15.230

Chapter 6

CONCLUSIONS

A three dimensional ray tracing computer program has been used to study the following effects of ionospheric propagation:

(a) Effect of elevation angle and frequency on HF radio waves through the ionosphere.

(b) Effects of ionospheric irregularities on ground-to-ground HF rays.

(c) Effects of ionospheric irregularities on Satellite-to-ground VHF rays.

(d) Phase path characteristics for oblique angle rays.

In addition computations were made to study the Doppler shift produced by motion of ionospheric irregularities.

The following conclusions may be drawn from the results of this simulation.

1. The ray path trajectories through an undisturbed ionosphere are symmetrical with respect to the point of reflection.

2. Ray path trajectories are significantly affected in the vicinity of the electron density irregularity. The irregularity model chosen was that of a torus; the rays whose wave reversals occur near the center of the torus are the most severely affected.

3. As the torus transmitter separation increases, the effect of torus on ground range and various path lengths increases and the effect is maximum when the torus is located near wave reversal point. It is observed that focussing of high angle radio waves with low angle radio ways, in the presence of torus, may result in increase or decrease in the amplitude of received signal.

4. The effect of the torus on VHF signal transmitted from satellite is insignificant.

5. The Phase Path versus Ground Range characteristic for various elevation angles has a zero slope for elevation angle 90°.

6. For frequency of operation greater than vertical critical frequency the low angle and high angle branches of the curve, phase path (P) versus ground range (D), meet in a cusp. A plot of group path (P') against ground range (D) shows a 'nose' near the skip distance.

7. The slope of the (P,D) curve does not undergo any large changes near the cusp, whereas that of (P',D) curve changes rapidly round the nose.

8. There was no noticeable Doppler shift for satellite-to-ground waves at 41 MHz when the torus velocity was taken as 160 m/sec.

Various other topics such as phase distortion of UHF signal, absorption, Doppler shift, focussing and

defocussing of radio waves due to ionospheric irregularities can be studied using ray tracing techniques. For complete ionospheric probing a reader should also consider the effect of lower atmosphere (troposphere) particularly when considering frequencies in the microwave band. The communication from satellite to another satellite can be studied in which case Doppler effect will be of importance.

REFERENCES

1. Budden, K.G., 'Radio Waves in the Ionosphere', Cambridge University Press, New York, 1966.

2. Davies, Kenneth, 'Ionospheric Radio Propagation', Dover Publication, Inc. New York, 1966.

3. Davies, Kenneth, 'Ionospheric Radio Waves', Blaisdell Publishing Company, University of Colorado, 1968.

4. Gething, P.J.D., 'Relation between Oblique and Ground Path-lengths in Ionospheric Propagation over a Curved-Earth', Nature, Lond. 193, 260, 1962.

5. Gething, P.J.D., 'Relationship between Phase Path and Effective Path for Oblique Ionospheric Propagation', J. atmos. terr. Phys., 27, 57, 1965.

6. Gething, P.J.D., 'Phase Path Characteristics for Oblique Ray Paths', J. atmos. terr. Phys., Vol.36, pp. 1-8, 1974.

7. Haselgrove, J., 'Ray Theory and New Method of Ray Tracing', London Physical Society, Report of Conference on the Physics of the Ionosphere, 1954.

8. Heisler, L.H., 'Observation on Movement of Perturbations in the F-region', J. atmos. terr. Phys., Vol.25, 1, 71-86, 1963.

9. Jones, R.M., 'A Three-Dimensional Ray Tracing Computer Program', ESSA Tech. Rept. IER17-ITSA17, 1966.

10. Jones, R.M., 'Modification to the Three-Dimensional Ray Tracing Program' described in IER17-ITSA17, 1968.

11. Jordan, E.C., 'Electromagnetic Waves and Radiating Systems', Prentice Hall, 1969.

12. Kelso, J.M., 'Ray Tracing in the Ionosphere', Radio Sci., Vol.3, (New Series), No.1, pp. 1-11, Jan. 1968.

13. Munro, G.H., 'Travelling Disturbances in the Ionosphere', Proc. Roy.Soc., London, 202A, 208-223, 1950.

14. Munro, G.H., 'Travelling Disturbances in the F-Region', Australian J. Phys., 11, 91-112, 1958.

15. Singh, Sarabjit, 'Computerised Three Dimensional Ray Tracing in the Ionosphere', M.Tech. Thesis, Department of Electrical Engineering, Indian Institute of Technology, Kanpur, 1972.

16. Titheridge, J.E., 'Large Scale Irregularities in the Ionosphere', J. Geophys. Res., 68, 3399, 1963.

17. Titheridge, J.E., Stuart, G.F., 'The Height of Large Ionospheric Irregularities', J. atmos.terr. Phys., Vol.28, pp. 255-258, 1966.

18. Titheridge, J.E., 'The Characteristics of Large Ionospheric Irregularities', J. atmos. terr. Phys., Vol.36, pp. 73-84, 1968.

EE-1974-M-PAN-RAY.